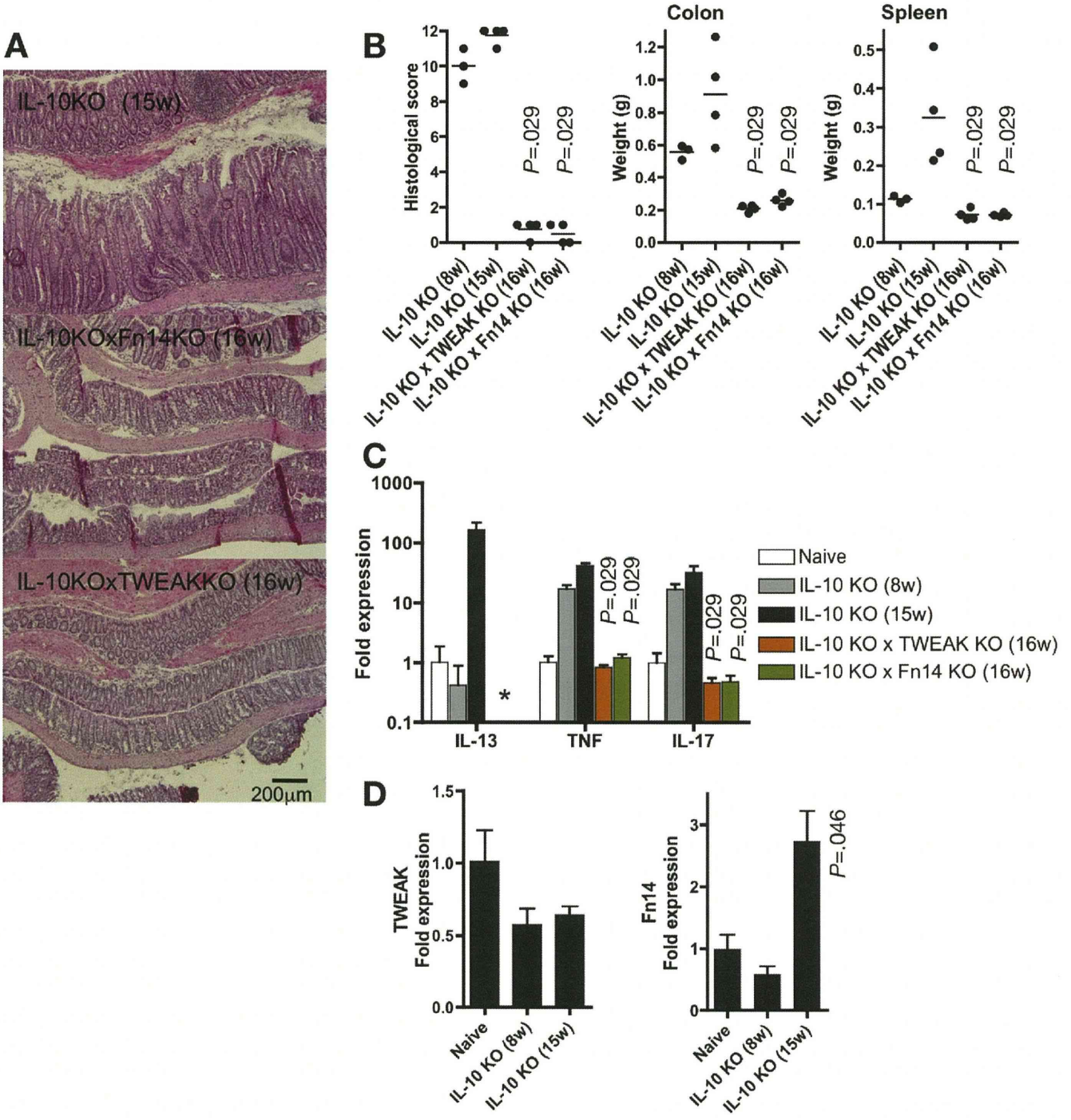

Figure 6. TWEAK/Fn14-mediated spontaneous colitis in IL-10 KO mice. (*A*) Representative section of the colon stained with H&E. (*B*) Histologic score, weight of colon and spleen. Each *symbol* represents an individual animal. (*C*) Cytokine mRNA levels in total colon tissue shown as relative expression to WT naïve colon. See Supplementary Materials and Methods for details. *Signal for IL-13 was not detected in any IL-10 KO × TWEAK KO and IL-10 KO × Fn14 KO mice. (*D*) TWEAK and Fn14 mRNA expression in IL-10 KO mice. *P* values are shown for significant differences between (*B* and *C*) IL-10 KO (15 w [weeks old]) and double KO mice (16w) and between (*D*) naïve and IL-10 KO 15w mice.

We found that IL-13–induced apoptosis was comparable to that induced by exogenous TNF-α. Although mRNA for Fn14 and TNF-α is at relatively low levels in normal colon, Fn14 and TNF-α protein is apparently sufficiently expressed in the explants, as evidenced by the fact that the Fn14- and TNF-α–dependent apoptosis induced by exogenous IL-13 does not require new protein synthesis. IL-13 has been reported to induce shedding of transforming growth factor α in bronchial epithelial cells, which is mediated by TACE.[21] In this cell line, IL-13 changes intracellular localization of transforming growth factor α from cytoplasm to apical side, where ADAM17 activity is high. Although speculative, it is possible that IL-13 induces a change in the localization of TWEAK, Fn14, and/or TNF-α. In addition, in tumor cell lines, TWEAK was shown to induce TNF-α expression and also TNF-α secretion into culture supernatants,[13,22] which

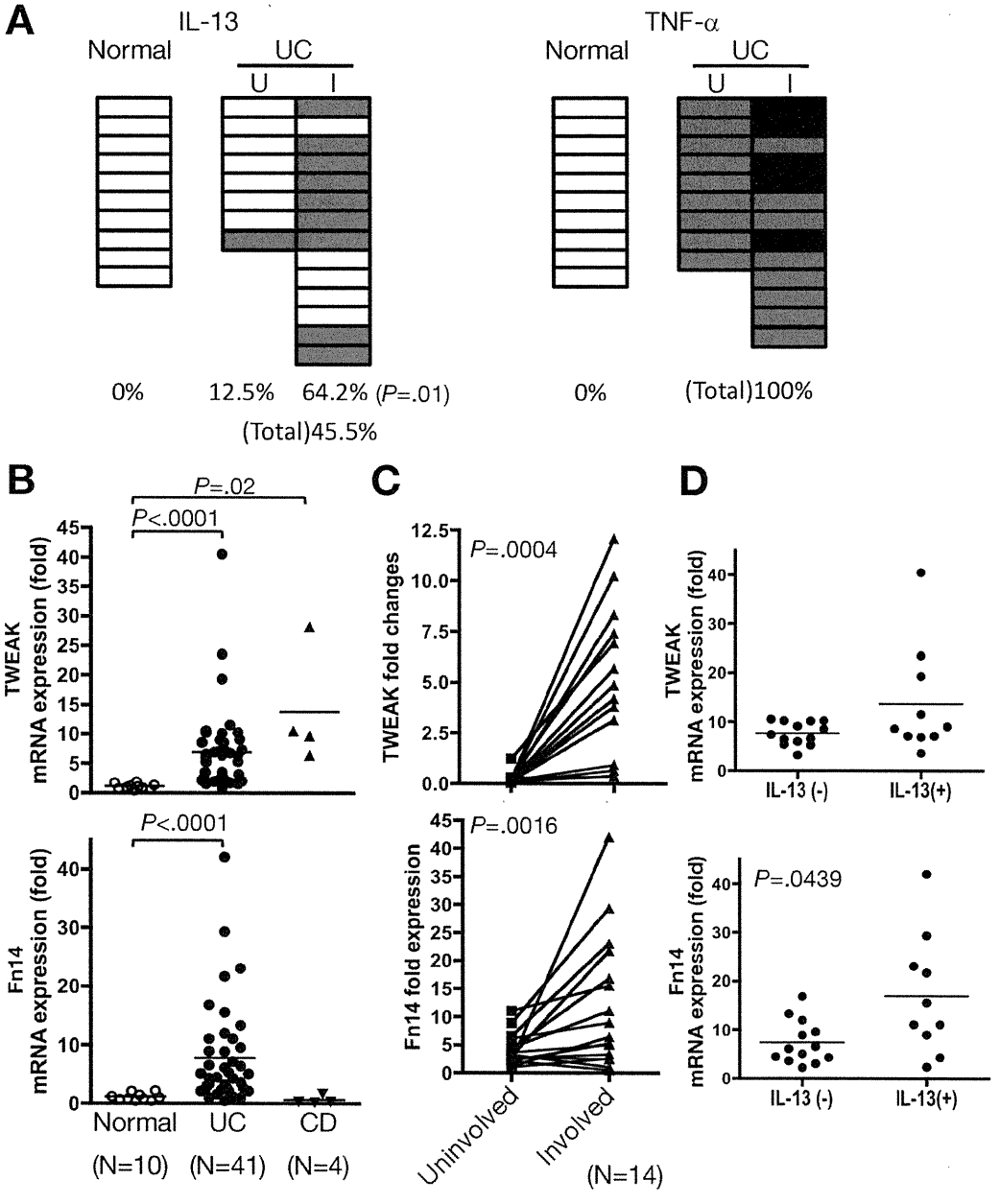

Figure 7. IL-13, TWEAK, and Fn14 are up-regulated in the inflamed mucosa of patients with UC. RNA extract from surgically resected colon mucosa was subjected to quantitative reverse-transcription polymerase chain reaction for IL-13, TWEAK, and Fn14. (*A*) Expression of IL-13 and TNF-α. *Open bars*, sample where transcripts were not detected after 40 cycle of polymerase chain reaction; *gray boxes*, samples with detectable mRNA; *black boxes*, samples with more than 2-fold increase when compared with paired uninvolved mucosa. Paired squares indicate uninvolved mucosal sample (U) and involved mucosal sample (I) obtained from the same patient. Percentage of mRNA-positive samples is as indicated at the bottom. The difference in the frequency of IL-13 expression between U and I group was statistically significant (χ^2 test). (*B*) Expression level of TWEAK and Fn14 expressed relative to the average signal value of normal colon is shown. *Horizontal lines* indicate mean value. (*C*) Paired samples of uninvolved mucosa and involved mucosa from patients with UC are compared. Paired *t* test was used for statistical analysis. (*D*) Samples in *panel A* separated into IL-13–positive or –negative groups and the levels of TWEAK and Fn14 were compared.

may relate to our finding of TWEAK-dependent TACE activation and TNF-α shedding. A report that TACE activity is up-regulated in UC mucosa but not Crohn's disease also supports the relevance of our finding.[23] Further studies are needed to delineate the signaling events downstream of IL-13 that lead to TWEAK/Fn14-dependent TACE-mediated TNF-α shedding. However, once the process is started, these pathways act interdependently to promote IEC apoptosis, destroying the mucosal barrier and increasing exposure to bacterial stimulation from the lumen, thereby promoting the recruitment and activation of inflammatory cells. This is a powerful mechanism to perpetuate and aggravate intestinal inflammation, which may play a significant role in chronic colitis in IL-10 KO mice as well as human UC. As the natural course in IL-10 KO mice, we found that IL-13 and Fn14 up-regulation were not seen until they were in the ex-SPF facility for 9 weeks (15 weeks old). We speculate that at the onset of colitis, TNF-α supported by TWEAK/Fn14

was the major player, and then the IL-13-TWEAK/Fn14 axis is added in chronic phase, destroying the epithelial integrity, which results in more bacterial translocation and splenomegaly. Although a recent report showed the protective effect of IL-13 in IL-10 KO mice,[24] their system was not natural spontaneous colitis but modified by administration of toxin and infection with parasites. Thus, we believe the latter result is not conflicting with our study.

Previous reports that the TWEAK/Fn14 pathway augments TNF-α apoptotic signaling[13,14,22] is consistent with our new observation that IL-13–induced TWEAK/Fn14-dependent cell death occurs via TNF-α, as well as our finding that exogenous TNF-α–induced IEC death was partially dependent on TWEAK/Fn14. Thus, TWEAK/Fn14 can function as a promoter of IEC damage in the presence of IL-13 or TNF-α. However, its mechanism seems to be distinct from those in previous reports where TWEAK signaling promotes TNF-α synthesis, as well as degradation of cIAP1, which suppresses TNF-α–induced nuclear factor κB activation.[13,22] In our study, de novo protein synthesis is not required, and cIAP1 is possibly not involved in the promotion of caspase activation by IL-13 treatment in WT IECs, because cIAP1 protein levels were higher in WT as compared with Fn14 KO tissue (data not shown).

Thus, we showed the cross talk between IL-13 and TWEAK/Fn14 signaling; however, we still do not know precisely how this occurs. Of note, IL-13–induced IEC damage occurs in the tissue from IL-4 receptor–deficient mice, and IL-4 failed to induce caspase activation in WT mice. These results indicate that IL-13–induced cell damage may not be mediated by the known IL-13 signaling receptor, which is a heterodimer of IL-4 receptor and IL-13 receptor α1, shared with IL-4. It is possible that IL-13 receptor α1 or IL-13 receptor α2 might function to transduce an IL-13 signal.[25–27] We speculate that the cross talk between IL-13 and TWEAK/Fn14 pathways occurs at the level of intracellular signaling, because it is unlikely that there is a molecular interaction at the extracellular level between IL-13 and its receptor(s) and the Fn14/TWEAK system (E. Day, Biogen Idec, personal communication, March 2011).

The tissue damage after γ-irradiation is mainly triggered by oxidative stress–induced DNA damage, followed by activation of the p53 pathway and cell cycle arrest. Increased oxidative stress associated with epithelial cell injury[28] and DNA damage[29] in UC has been also reported. In UC, Fn14 may not only mediate IL-13–induced IEC death, but may further enhance DNA damage by induction of proinflammatory mediators, resulting in the recruitment of reactive oxygen species–producing macrophages and neutrophils. Following DNA damage may be the induction of p21 and cell cycle checkpoint arrest and accelerated cell death. Thus, once IL-13, TWEAK/Fn14, and TNF-α are all involved in the inflammatory cascade, there is a strong cooperation in place to enhance inflammation and IEC damage. This mechanism is the probable cause of irradiation-induced gastrointestinal syndrome and also the rapid and wide-ranging IEC loss in patients with fulminant UC. Anti–TNF-α monoclonal antibody has recently become available for treatment of UC. Based on our studies, neutralizing TWEAK or IL-13 may be potential new therapies for UC, and combination of anti-TWEAK or anti–IL-13 antibodies with anti–TNF-α antibody might be beneficial for the treatment or prevention of resistance to anti–TNF-α therapy.

In the clinical aspect, developing colon cancer is also a significant factor that determines the prognosis of UC. Blocking TNF-α has clearly reduced tumor formation in the mice system.[30,31] We have previously shown that the Th2-dominant immune response promoted inflammation-related tumorigenesis in the colon.[32] A recent report, which describes that IL-4 and IL-13 enhance the expression of activation-induced cytidine deaminase in colonic cells evoking genetic mutations in the TP53 gene,[33] supports this notion. These findings suggest the beneficial effect of neutralization of IL-13 in UC to prevent cancer development as well.

Our present study shows that the TWEAK/Fn14 pathway is involved in both TNF-α and IL-13–induced IEC death. This is a crucial mechanism in intestinal mucosal injury induced by γ-irradiation, as well as inflammation where either IL-13 or TNF-α is up-regulated. Blockade of TWEAK or IL-13 alone, or in combination with anti–TNF-α may be useful to treat UC. It also may prevent radiation-induced gastrointestinal injury for which there are no countermeasures today.

Supplementary Materials

Note: To access the supplementary material accompanying this article, visit the online version of *Gastroenterology* at www.gastrojournal.org, and at doi:10.1053/j.gastro.2011.08.040.

References

1. Heller F, Fromm A, Gitter AH, et al. Epithelial apoptosis is a prominent feature of the epithelial barrier disturbance in intestinal inflammation: effect of pro-inflammatory interleukin-13 on epithelial cell function. Mucosal Immunol 2008;1(Suppl 1):S58–S61.
2. Schulzke JD, Ploeger S, Amasheh M, et al. Epithelial tight junctions in intestinal inflammation. Ann N Y Acad Sci 2009;1165:294–300.
3. Kawashima R, Kawamura YI, Kato R, et al. IL-13 receptor α2 promotes epithelial cell regeneration from radiation-induced small intestinal injury in mice. Gastroenterology 2006;131:130–141.
4. Heller F, Florian P, Bojarski C, et al. Interleukin-13 is the key effector Th2 cytokine in ulcerative colitis that affects epithelial tight junctions, apoptosis, and cell restitution. Gastroenterology 2005;129:550–564.
5. Fuss IJ, Heller F, Boirivant M, et al. Nonclassical CD1d-restricted NK T cells that produce IL-13 characterize an atypical Th2 response in ulcerative colitis. J Clin Invest 2004;113:1490–1497.
6. Fuss IJ, Strober W. The role of IL-13 and NK T cells in experimental and human ulcerative colitis. Mucosal Immunol 2008;1(Suppl 1):S31–S33.
7. Strober W, Kitani A, Fichtner-Feigl S, et al. The signaling function of the IL-13Ralpha2 receptor in the development of gastrointestinal fibrosis and cancer surveillance. Curr Mol Med 2009;9:740–750.
8. Kaplan MJ, Lewis EE, Shelden EA, et al. The apoptotic ligands TRAIL, TWEAK, and Fas ligand mediate monocyte death induced by autologous lupus T cells. J Immunol 2002;169:6020–6029.

9. Maecker H, Varfolomeev E, Kischkel F, et al. TWEAK attenuates the transition from innate to adaptive immunity. Cell 2005;123: 931–944.
10. Burkly LC, Michaelson JS, Hahm K, et al. TWEAKing tissue remodeling by a multifunctional cytokine: role of TWEAK/Fn14 pathway in health and disease. Cytokine 2007;40:1–16.
11. Brown SA, Richards CM, Hanscom HN, et al. The Fn14 cytoplasmic tail binds tumour-necrosis-factor-receptor-associated factors 1, 2, 3 and 5 and mediates nuclear factor-kappaB activation. Biochem J 2003;371:395–403.
12. Saitoh T, Nakayama M, Nakano H, et al. TWEAK induces NF-kappaB2 p100 processing and long lasting NF-kappaB activation. J Biol Chem 2003;278:36005–36012.
13. Vince JE, Chau D, Callus B, et al. TWEAK-FN14 signaling induces lysosomal degradation of a cIAP1-TRAF2 complex to sensitize tumor cells to TNFalpha. J Cell Biol 2008;182:171–184.
14. Wicovsky A, Salzmann S, Roos C, et al. TNF-like weak inducer of apoptosis inhibits proinflammatory TNF receptor-1 signaling. Cell Death Differ 2009;16:1445–1459.
15. Dohi T, Borodovsky A, Wu P, et al. TWEAK/Fn14 pathway: a nonredundant role in intestinal damage in mice through a TWEAK/intestinal epithelial cell axis. Gastroenterology 2009;136:912–923.
16. Campbell S, Burkly LC, Gao HX, et al. Proinflammatory effects of TWEAK/Fn14 interactions in glomerular mesangial cells. J Immunol 2006;176:1889–1898.
17. Jakubowski A, Ambrose C, Parr M, et al. TWEAK induces liver progenitor cell proliferation. J Clin Invest 2005;115:2330–2340.
18. Chicheportiche Y, Bourdon PR, Xu H, et al. TWEAK, a new secreted ligand in the tumor necrosis factor family that weakly induces apoptosis. J Biol Chem 1997;272:32401–32410.
19. Grossmann J, Walther K, Artinger M, et al. Apoptotic signaling during initiation of detachment-induced apoptosis ("anoikis") of primary human intestinal epithelial cells. Cell Growth Differ 2001; 12:147–155.
20. Strober W, Fuss IJ. Proinflammatory cytokines in the pathogenesis of inflammatory bowel diseases. Gastroenterology 2011;140: 1756–1767.
21. Booth BW, Sandifer T, Martin EL, et al. IL-13-induced proliferation of airway epithelial cells: mediation by intracellular growth factor mobilization and ADAM17. Respir Res 2007;8:51.
22. Ikner A, Ashkenazi A. TWEAK induces apoptosis through a death-signaling complex comprising receptor-interacting protein 1 (RIP1), Fas-associated death domain (FADD), and caspase-8. J Biol Chem 2011;286:21546–21554.
23. Brynskov J, Foegh P, Pedersen G, et al. Tumour necrosis factor alpha converting enzyme (TACE) activity in the colonic mucosa of patients with inflammatory bowel disease. Gut 2002;51:37–43.
24. Wilson MS, Ramalingam TR, Rivollier A, et al. Colitis and intestinal inflammation in IL10-/- mice results from IL-13Ralpha2-mediated attenuation of IL-13 activity. Gastroenterology 2011; 140:254–264.
25. Fichtner-Feigl S, Strober W, Kawakami K, et al. IL-13 signaling through the IL-13alpha2 receptor is involved in induction of TGF-beta1 production and fibrosis. Nat Med 2006;12:99–106.
26. Mandal D, Fu P, Levine AD. REDOX regulation of IL-13 signaling in intestinal epithelial cells: usage of alternate pathways mediates distinct gene expression patterns. Cell Signal 2010;22:1485–1494.
27. Mandal D, Levine AD. Elevated IL-13Ralpha2 in intestinal epithelial cells from ulcerative colitis or colorectal cancer initiates MAPK pathway. Inflamm Bowel Dis 2010;16:753–764.
28. McKenzie SJ, Baker MS, Buffinton GD, et al. Evidence of oxidant-induced injury to epithelial cells during inflammatory bowel disease. J Clin Invest 1996;98:136–141.
29. Roessner A, Kuester D, Malfertheiner P, et al. Oxidative stress in ulcerative colitis-associated carcinogenesis. Pathol Res Pract 2008;204:511–524.
30. Onizawa M, Nagaishi T, Kanai T, et al. Signaling pathway via TNF-alpha/NF-kappaB in intestinal epithelial cells may be directly involved in colitis-associated carcinogenesis. Am J Physiol Gastrointest Liver Physiol 2009;296:G850–G859.
31. Popivanova BK, Kitamura K, Wu Y, et al. Blocking TNF-alpha in mice reduces colorectal carcinogenesis associated with chronic colitis. J Clin Invest 2008;118:560–570.
32. Osawa E, Nakajima A, Fujisawa T, et al. Predominant T helper type 2-inflammatory responses promote murine colon cancers. Int J Cancer 2006;118:2232–2236.
33. Endo Y, Marusawa H, Kou T, et al. Activation-induced cytidine deaminase links between inflammation and the development of colitis-associated colorectal cancers. Gastroenterology 2008; 135:889–898, 898 e1–3.

Received December 12, 2010. Accepted August 23, 2011.

Reprint requests

Address requests for reprints to: Taeko Dohi, MD, PhD, Department of Gastroenterology, Research Center for Hepatitis and Immunology, Research Institute, National Center for Global Health and Medicine, 1-21-1 Toyama, Shinjuku-ku, Tokyo 162-8655, Japan. e-mail: dohi@ri.ncgm.go.jp; fax: (81) 3-3202-7364.

Acknowledgments

L.C.B. and T.D. share senior authorship.

The microarray files and information have been uploaded to the National Center for Biotechnology Information GEO public repository (accession number GSE25029).

Conflicts of interest

The authors disclose no conflicts.

Funding

Supported in part by grants and contracts from the program Grants-in-Aid for Scientific Research (B) and Grants-in Aid for Young Scientists (B) from the Ministry of Education, Cultures, Sports, Science, and Technology; the Grant of National Center for Global Health and Medicine (21-110, 22-205), the Ministry of Health, Labor, and Welfare; Japan Health Sciences Foundation and Organization; and Health and Labor Sciences Research Grants for research on intractable diseases from the Ministry of Health, Labor and Welfare of Japan.

Supplementary Materials and Methods

Mice, γ-Irradiation Protocol, and Induction of Colitis

TWEAK or Fn14 KO mice were backcrossed onto BALB/c or C57BL/6 backgrounds for 5 to 6 generations under SPF conditions. Mice with BALB/c background were used in this study, except crossing IL-10 KO mice. Mice received whole body irradiation using the γ-irradiation apparatus MBR-1520-R (Hitachi Medical Corp, Tokyo, Japan). IL-10 KO mice with C57BL/6 background were obtained from The Jackson Laboratory and maintained in our facility. TWEAK and IL-10 double KO mice and Fn14 and IL-10 double KO mice were generated by crossing TWEAK KO mice or Fn14 KO mice with C57BL/6 background with IL-10 KO mice. All mice bred and maintained in our SPF facility were free from signs of enteritis. We have an area separated from SPF in our animal facility (ex-SPF), where clean SPF-level mice are carried in and kept in the same way as in the SPF area, with sterile cages, drinking water, food, and controlled temperature and humidity, except a HEPA filter is not equipped in the air conditioning system. In addition, cages in the ex-SPF area are not placed in racks with a HEPA filter as they are in the SPF area but in open racks. Therefore, the atmosphere in the ex-SPF area is different from our SPF area. On microbiological examination, no major pathogens have been detected in the ex-SPF area. When IL-10 KO mice were moved from the SPF to ex-SPF area, they showed transient anal prolapse on defecation with soft feces within 4 weeks; thus, for our experimental study, female mice born within a month from each of the 3 strains were moved from the SPF to ex-SPF area at the age of 6 weeks. All experimental protocols were approved by the local institutional animal care and use committees.

Reagents

Murine anti-TWEAK antibody P2D10, murine TNF receptor immunoglobulin (Ig), and the murine control antibody clone P1.17 were prepared by Biogen Idec. IL-13 receptor α2-Ig (IL-13Rα2-Ig) was previously described.[1] Control human IgG was purchased from Rockland Immunochemicals (Gilbertsville, PA).

Microcolony Survival Assay

Mice were given 12 Gy or γ-irradiation on day 0; on day 6, 7-cm lengths of the jejunum and the ileum and whole colon were resected. Tissues were opened longitudinally, fixed in 10% formalin overnight, rolled, and then embedded in paraffin to prepare sections, including whole length of specimens. After H&E staining, numbers of microcolonies of regenerating crypts with more than 10 cells in each section were enumerated.

Analysis of Affymetrix Data

Throughout the Affymetrix analysis, colon and jejunum data were analyzed and considered separately. Affymetrix scans were subject to quality control measures. These tests included a visual inspection of the distribution of raw signal intensities and an assessment of RNA degradation, relative log expression, and normalized unscaled standard error. All sample scans passed these quality control metrics.

CEL files were subjected to GC content-based robust multi-array average (GCRMA) normalization.[2,3] Expression levels were log (base 2) transformed. All calculations and analyses were performed using R and Bioconductor computational tools.[4]

Analyses were applied to discover genes that were differentially expressed (DEGs) in colon and jejunum between γ-irradiated animals and control-treated animals of the same genotype. To identify differentially expressed genes between groups of samples, we applied the linear modeling approach to fit gene expression levels ($\log_2$ transformed) according to the defined groups of samples and Bayesian posterior error analysis as implemented by Smyth.[5] Genes that exhibited a log-odds score (lods) greater than zero and fold change greater then 1.5 were considered significantly different. In the colon, γ-irradiated WT animals exhibited 170 and 249 DEGs over control at 6 hours and 24 hours, respectively. In the jejunum, these numbers were 98 and 156. In the colon, γ-irradiated KO animals exhibited 131 and 43 DEGs over control at 6 hours and 24 hours, respectively. In the jejunum, these numbers were 131 and 116.

The Affymetrix annotation file was used to identify those probe sets that are involved in "Mitosis," "Cell Cycle," or "Apoptosis" according to the Gene Ontology Biological Process annotation. To assess whether these particular biological functions were overrepresented in this study, a hypergeometric test was performed and showed that, in the colon, mitosis, cell cycle, and apoptosis were overrepresented with *P* values of 1.3e-29, 7.9e-39, and 6.9e-08, respectively. In jejunum, these *P* values were 1.6e-08, 1.3e-10, and .0004.

The microarray files and information have been uploaded to the National Center for Biotechnology Information GEO public repository (accession number GSE25029).

Effect of Exogenous TWEAK In Vivo

BALB/c WT or Fn14 KO mice were injected with murine Fc-TWEAK, 200 mg per dose by intraperitoneal route, according to various dose regimens as follows: injection on day 0 and death on day 3, injection on days 0, 3, and 7 and death on day 10, or injection on days 0, 3, 7, 10, and 17 and death on day 18. Two hours before the mice were killed, each mouse was injected intraperitoneally with bromodeoxyuridine (BrdU) 1.5 mg/10 g body wt. The gastrointestinal tract was removed and

Supplementary Table 1. Histologic Scoring System

Score	0	1	2
Loss of goblet cells	None	Focal	Diffuse
Crypt elongation	None	~1.5-fold of normal tissue	More than 1.5-fold
Cell infiltration	None	Infiltration mainly limited in the mucosal layer without obvious space between crypts	Infiltration into the mucosal layer forming wide space between crypts or with infiltration in submucosal layer

flushed with phosphate-buffered saline (PBS), and the duodenum, jejunum, ileum, and colon were each cut into 2 segments, one of which was processed as follows. Segments were laid straight on dry filter paper, cut longitudinally with dull pointed scissors to open them, fixed in 4% paraformaldehyde (PFA), and paraffin embedded, and sections of 5-μm thickness stained with H&E or immunohistochemically stained for BrdU (monoclonal mouse anti-BrdU; DakoCytomation Denmark A/S, Glostrop, Denmark) and caspase-3 (polyclonal rabbit anti-caspase-3; Biocare Medical, LLC, Concord, CA). Efficacy of this dose regimen was confirmed by induction of oval cell proliferation in the liver, consistent with the previously reported oval cell proliferation in TWEAK-overexpressing mice.[6]

Real-Time Polymerase Chain Reaction

Total RNA was prepared from whole mucosa or primary culture tissue by using RNA-Bee RNA isolation solvent (Tel-Tests, Inc, Friendswood, TX). Complementary DNA was synthesized from RNA by reverse transcription. The polymerase chain reaction (PCR) primers used were as follows: murine glyceraldehyde-3-phosphate dehydrogenase (GAPDH), 5′-AGCCAAACGGGTCATCATCTC and 5′-TGCCTGCTTCACCACCTTCTT;. Primers and probes for mouse TWEAK and Fn14 are described elsewhere.[6] Primers and probes from human IL-13, TWEAK, and Fn14 were purchased (Applied Biosystems, Warrington, England). The step-cycle program was annealing at 60°C for 45 seconds and extension at 72°C for 45 seconds for a total of 40 cycles. Expression of mRNA was assessed by quantitative PCR using a SYBR Green PCR Master Mix (Applied Biosystems) and ABI PRISM 7900 Sequence Detector (Applied Biosystems). Threshold cycle numbers (Ct) were determined with Sequence Detector Software (version 1.7; Applied Biosystems) and transformed by using the DCt/DDCt method as described by the manufacturer, with GAPDH used as the calibrator gene.

Separation and Culture of Purified Crypt

Small intestine were rinsed in PBS and then treated with 30 mmol/L EDTA in PBS for 40 minutes at room temperature while exchanging the solutions every 5 minutes. The supernatant was collected in fractions for 25 to 40 minutes, centrifuged (1 minute at 300*g*), and washed with i-PIPES buffer with antibiotics. The 100 released crypts per tube were put in i-PIPES buffer with antibiotics in siliconized tubes. The crypts were then incubated for 4 hours for 37°C with 40 ng/mL of recombinant IL-13 (PeproTech Inc). The crypts were washed with i-PIPES buffer with antibiotics, put on the slide glass, dried, and fixed with 4% PFA in PBS for 15 minutes at room temperature.

Histologic Analysis

Formalin-fixed, paraffin-embedded sections were heated with 10 mmol/L citric buffer at 121°C for 10 minutes, blocked with 10% normal rabbit serum, and stained with mouse anti-β-catenin monoclonal antibody (BD Biosciences, San Jose, CA) and biotin-labeled anti-mouse IgG antibody (Nichirei, Tokyo, Japan) followed by streptavidin/fluorescein isothiocyanate (BD PharMingen, San Diego, CA). The frozen sections were dried, fixed with 4% PFA in PBS for 15 minutes at room temperature, unmasked as previously described, and treated with 0.5% bovine serum albumin in PBS for 30 minutes and anti-ZO-1 (Zymed Laboratories, South San Francisco, CA) for 2 hours at room temperature, followed by tetramethylrhodamine isothiocyanate–labeled anti-rabbit IgG antibody (SouthernBiotech, Birmingham, AL). Images were captured with a fluorescence microscope (Olympus Corp, Tokyo, Japan). To detect apoptosis, formalin-fixed, paraffin-embedded sections were stained with the DeadEnd Colorimetric TUNEL System (Promega, WI). TUNEL staining–positive cells per crypt were enumerated in each section (10–20 crypts) and were converted to percentage of apoptotic cells per crypt. To analyze colitis in IL-10 KO mice, colon was opened longitudinally, rolled, and snap frozen in liquid N_2. Total RNA was extracted from a part of rolled colon and the rest was embedded in OCT compound to prepare frozen sections with H&E. Histologic scores were assigned to each segment as in Supplementary Table 1. Proximal and distal colon segments were scored individually, and these scores were summed to reach a total score for the entire colon. Thus, the total possible histologic score is 12.

Western Blot Analysis

Tissues were lysed with 10 mmol/L Tris-HCl, pH 7.5, 0.15 mol/L NaCl, 1% Triton X-100, 0.1% sodium deoxycholate, 0.1% sodium dodecyl sulfate, 1 mmol/L EDTA, and proteinase inhibitor cocktail on ice. Lysates were cleared by centrifugation, and protein concentration was determined with the DC Protein Assay (Bio-Rad Laboratories, Hercules, CA). The samples were boiled with an equal volume of Laemmli sample buffer (Bio-Rad Laboratories) for 5 minutes. A total of 10 μg of protein was applied to sodium dodecyl sulfate/polyacrylamide gel electrophoresis with a

10% to 20% gradient gel (XV Pantera Gel; DRC Co, Ltd, Tokyo, Japan) and transferred onto polyvinylidene difluoride membranes (Immobilon-P; Millipore, Billerica, MA). Protein blotted membranes were treated with BLOCK-ACE (Snow Brand Milk Products Co, Ltd, Hokkaido, Japan) for 1 hour at room temperature, incubated with following antibodies in PBS containing 0.1% Tween 20 (PBS-T) and 10% BLOCK-ACE for 2 hours at room temperature: anti-caspase-2 (BD Biosciences), anti-caspase-3 (BioVision Research Products, Mountain View, CA), anti-caspase-8 (BD Biosciences), anti-caspase-9 (BioVision Research Products), and β-actin (Cell Signaling Technology, Inc, Beverly, MA). After washing with Tris-buffered saline containing 0.1% Tween 20, the membrane was incubated in horseradish peroxidase-conjugated secondary antibody (The Jackson Laboratory) for 1 hour at room temperature. Detection of signal was performed with SuperSignal West Dura Extended Duration Substrate (Thermo Fisher Scientific Inc, Waltham, MA) and was exposed with LAS3000 (Fujifilm, Tokyo, Japan, Tokyo, Japan). To obtain β-actin normalized value of the signal, ImageJ software (National Institutes of Health) was used.

Caspase-3 Activity

Caspase-3 activity was quantified using a fluorometric immunosorbent enzyme assay kit purchased from Roche Diagnostics (Tokyo, Japan) following the vendor's protocol. Fluorescence was measured using Flexstation (ABI). Four to 6 identical cultures were performed, and data were shown as average of relative activity to WT tissue cultured without stimuli.

TNF-α Assay

TNF-α in culture supernatant was measured using an enzyme-linked immunosorbent assay kit (R&D Systems, Minneapolis, MN). As an inhibitor of ADAM17, TAPI-2 (Merck, Darmstadt, Germany) was used.

Statistical Analysis

The results were statistically analyzed by the Mann–Whitney test using Prism 4 software (GraphPad Software, Inc, La Jolla, CA), unless indicated in the legend.

Supplementary Results

Gene Transcript Expression Profiling

Both WT and TWEAK KO mice exhibited increased expression of an array of apoptosis pathway genes in the colon at 6 hours after irradiation as compared with their naïve cohorts, indicating that both WT and TWEAK KO mice are similarly susceptible to γ-irradiation DNA damage. Consistent with this, p53 pathway activity was apparent in both the WT and TWEAK KO mice after irradiation, as evidenced by increased expression of p53-inducible genes *ccng1* (cyclin G1), indicative of G_2/M arrest, and *mdm2*. These inductions were more pronounced and prolonged in the WT mice, and only WT mice showed significant induction of other p53-inducible cell cycle inhibitors, *cdkn1a* (p21) and *cdkn2b*, and of *trp53inp1*. WT tissue also exhibited a pattern of decreased expression of cell cycle genes related to DNA replication at 6 hours and DNA replication and mitosis at 24 hours, such as MCM family genes (*mcm2, 3, 7, 5, 6, and 10*), cyclins (*ccnb1, ccnb2, and ccna2*), kinesins (*kif11 and kif22*), and spindle protein (*nusap1*), indicating decreased cell division as compared with naïve mice. WT mice also exhibited increases in an array of apoptotic genes at 24 hours, whereas in TWEAK KO mice a narrower spectrum of apoptotic genes was induced as compared with naïve mice. In contrast, cell cycle genes were not altered in TWEAK KO mice after irradiation at either 6 or 24 hours and apoptotic genes were not altered at 24 hours as compared with naïve mice, reflecting epithelial cell survival at 6 hours and almost normal cell turnover at 24 hours after irradiation. For genes involved in DNA repair, both *polk* and *ercc5* increased significantly in both WT and TWEAK KO after γ-irradiation, and several other DNA repair genes decreased in WT mice after γ-irradiation (*Ung, Syce2, H2afx, Pttg1, Hmgb2*). Similar patterns of gene changes were observed in the jejunum (data not shown). These results show the significant role of the TWEAK/Fn14 pathway in stress-induced cell cycle arrest and subsequent cell death.

Spontaneous Colitis Model

All seven IL-10 KO mice started to show soft stool within 1 week, with 3 mice were killed 2 weeks after moving to the ex-SPF housing facility (at 8 weeks old) because of severe diarrhea. Four showed anal prolapse but were kept under observation until 15 weeks old. All IL-10 KO mice showed severe colitis as determined by thick colon with elongated crypts and cell infiltration, together with splenomegaly and enlarged sacral lymph nodes. In contrast, TWEAK KO × IL-10 KO mice and Fn14 KO × IL-10 KO mice in ex-SPF area until 16 weeks old were free from all signs of inflammation. Soft stool or anal prolapse also was not seen in any of them, and the colons were apparently normal in macroscopic and microscopic observation.

Supplementary References

1. Kawashima R, Kawamura YI, Kato R, et al. IL-13 receptor a2 promotes epithelial cell regeneration from radiation-induced small intestinal injury in mice. Gastroenterology 2006;131:130–141.
2. Irizarry RA, Bolstad BM, Collin F, et al. Summaries of Affymetrix GeneChip probe level data. Nucleic Acids Res 2003;31:e15.
3. Li C, Hung Wong W. Model-based analysis of oligonucleotide arrays: model validation, design issues and standard error application. Genome Biol 2001;2:research0032.
4. Gentleman R. Bioinformatics and computational biology solutions using R and Bioconductor. New York, NY: Springer Science+Business Media, 2005.
5. Smyth GK. Linear models and empirical bayes methods for assessing differential expression in microarray experiments. Stat Appl Genet Mol Biol 2004;3:Article3.
6. Jakubowski A, Ambrose C, Parr M, et al. TWEAK induces liver progenitor cell proliferation. J Clin Invest 2005;115:2330–2340.

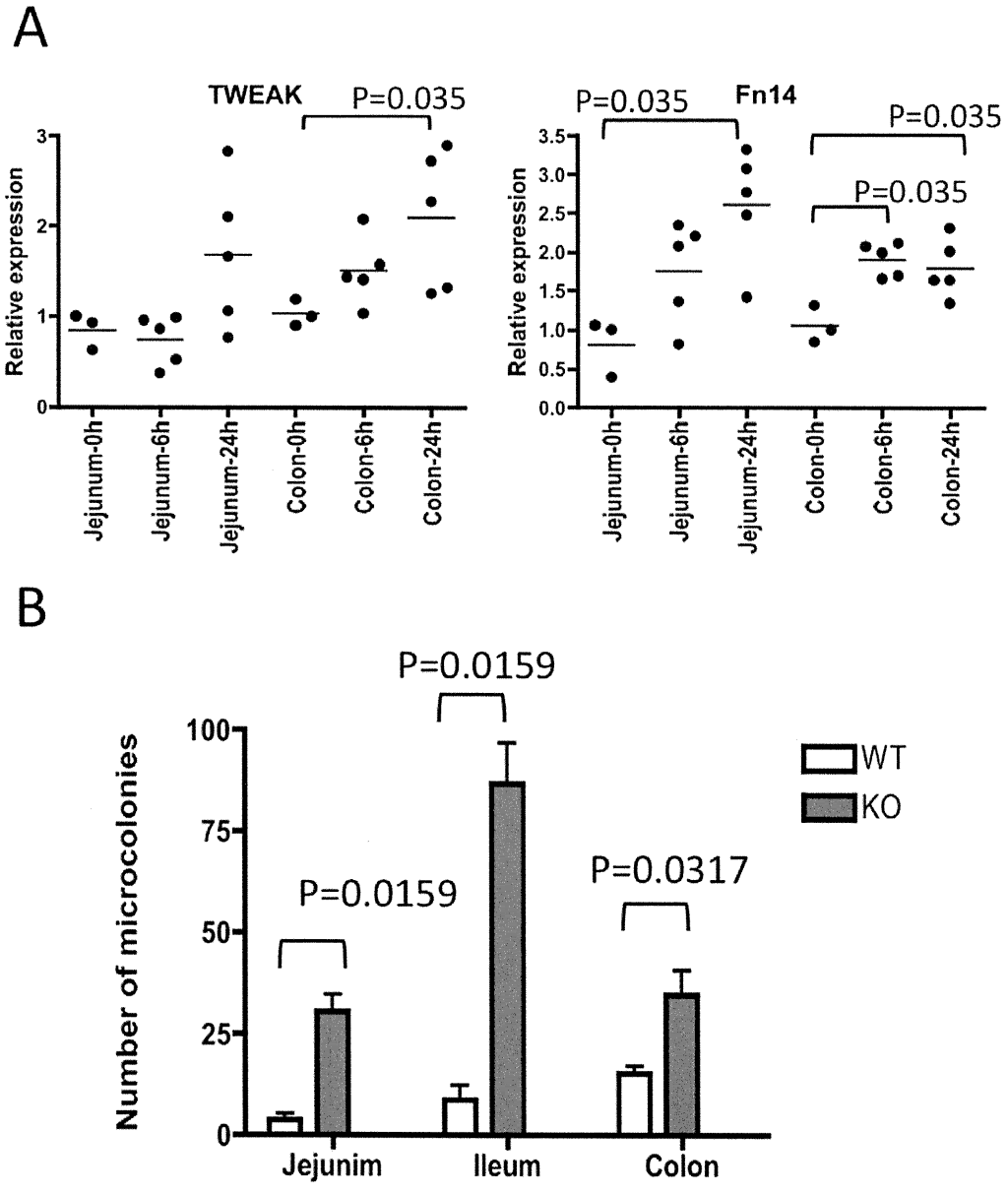

Supplementary Figure 1. TWEAK/Fn14 mediates γ-irradiation–induced cell death. (*A*) Expression of TWEAK, Fn14, and TNF-α in the whole tissue of jejunum and colon after 3-Gy γ-irradiation. Levels of mRNA were determined by quantitative reverse-transcription PCR normalized with GAPDH and demonstrated as fold change from one representative sample of naïve mice. *Horizontal bars* indicate mean values. (*B*) Number of microcolonies (regenerative epithelial cells) in the intestine of WT (n = 4) and Fn14 KO (n = 5) mice 6 days after 12-Gy γ-irradiation. Data are shown as mean ± SD.

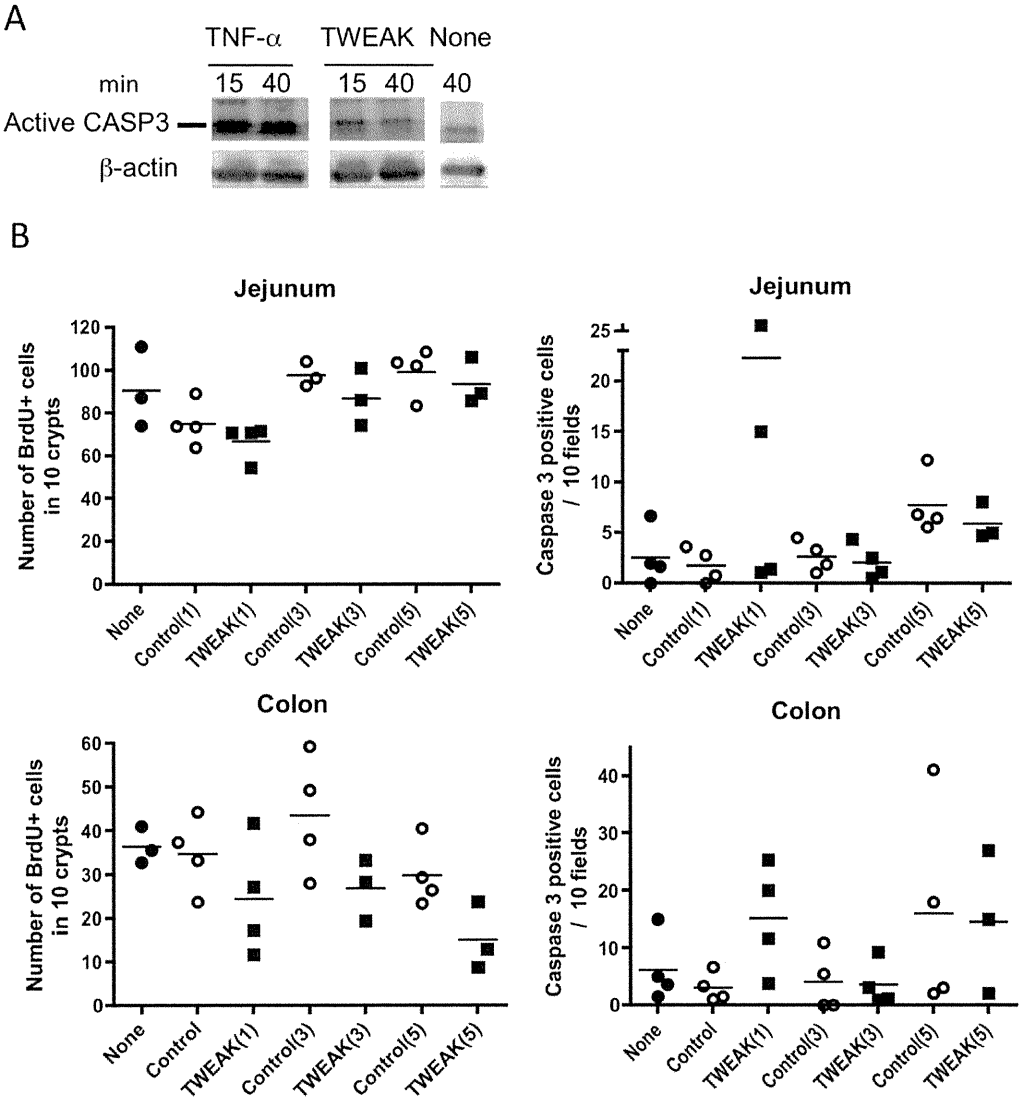

Supplementary Figure 2. TWEAK is a weak inducer of apoptosis of IECs. (*A*) Small intestines of WT BALB/c mice were taken and cultured in the presence of TNF-α or TWEAK. Protein extract at the indicated time in minutes was examined by Western blotting for caspase-3. (*B*) Numbers of BrdU-incorporated cells and caspase-3–positive cells in the intestine after intraperitoneal injection of TWEAK-Fc (TWEAK) or control antibody (control). None, no treatment. Numbers in *parentheses* indicate the number of injections of control or TWEAK: 1 indicates injection on day 0 and tissues obtained on day 1; 3 indicates injection on days 0, 3, and 7 and tissues obtained on day 10; and 5 indicates injection on days 0, 3, 7, 10, and 17 and tissues obtained on day 18. *Horizontal bars* indicate mean values.

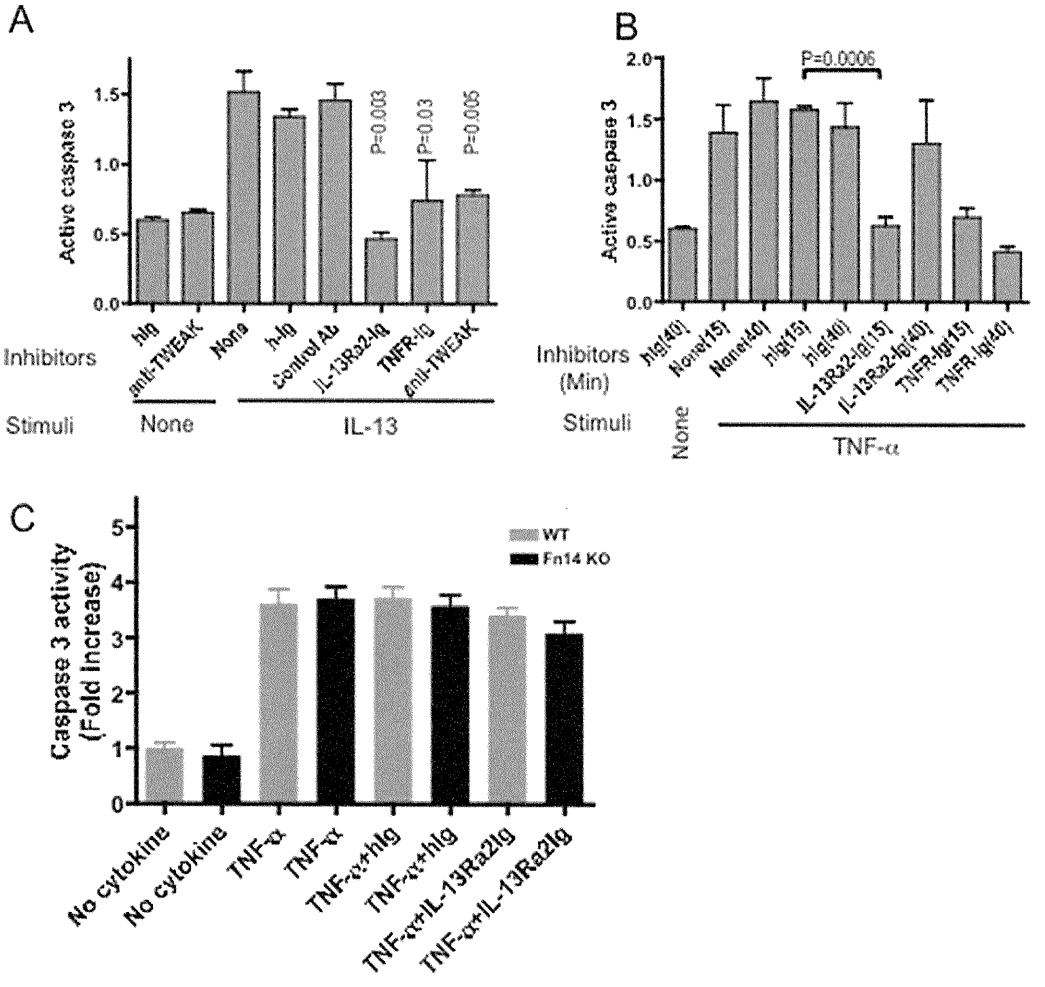

Supplementary Figure 3. IL-13–induced caspase activation is dependent on Fn14. Tissues were incubated in the presence of indicated cytokines or without cytokine (Control) for indicated times and protein extract was subjected to immunoblotting for caspases or assay for caspase-3 activity. (*A* and *B*) Tissues were prepared from WT mice and incubated with (*A*) IL-13 for 40 minutes or (*B*) TNF-α for the indicated time. Active caspase-3 was detected with Western blotting and quantified by densitometry with normalization with β-actin signal. Data from 3 independent experiments are shown as mean ± SD. (*C*) WT (*gray bars*) or Fn14 KO (*black bars*) tissues were incubated with TNF-α for 40 minutes with various inhibitors. Data from 5 independent cultures are shown as mean ± SD (relative to WT tissue with no cytokine). Inhibitors were added to the cultures as indicated to each lane of treatment, namely 5 μg/mL of murine anti-TWEAK antibody P2D10, murine TNF receptor-Ig (TNFR-Ig) or the murine control antibody clone P1.17 (Control Ab), IL-13 receptor α2-Ig (IL-13Ra2-Ig) or its control human IgG (hIg), or none. In *A–C*, Student *t* test was performed and *P* values are shown for significant differences between inhibitor and its control reagent.

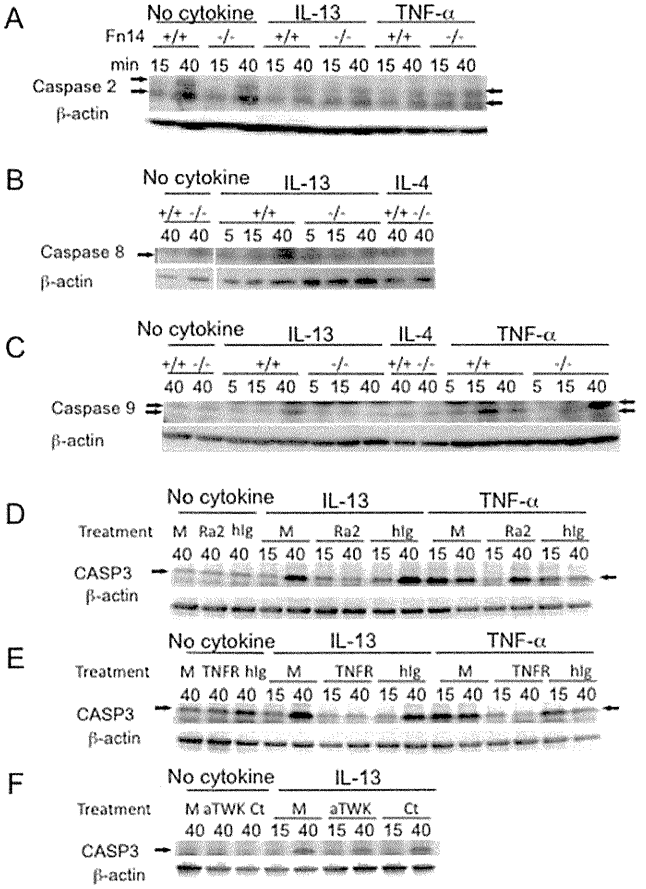

Supplementary Figure 4. IL-13–induced caspase activation is dependent on Fn14. Small intestinal tissue was incubated in the presence of indicated cytokines or without cytokine (Control) for indicated times (5, 15, or 40 minutes) and protein extract was subjected to immunoblotting for caspases. Tissues were prepared from WT or Fn14 KO mice and incubated with IL-13, IL-4, or TNF-α. Blotted membrane was probed with (*A*) anti-activated caspase-2, (*B*) caspase-8, (*C*) caspase-9, or (*D–F*) caspase-3. In *D–F*, tissues were prepared from WT mice and incubated with IL-13 or TNF-α or without (Control). Lanes of treatment indicates culture incubation with media alone (M), IL-13 receptor α2-Ig (Ra2) or its control human IgG (hIg), TNF receptor-Ig (TNFR), anti-TWEAK antibody P2D10 (aTWK), or control antibody clone P1.17 (Ct). Concentrations of antibodies and chimeric proteins are all 5 μg/mL.

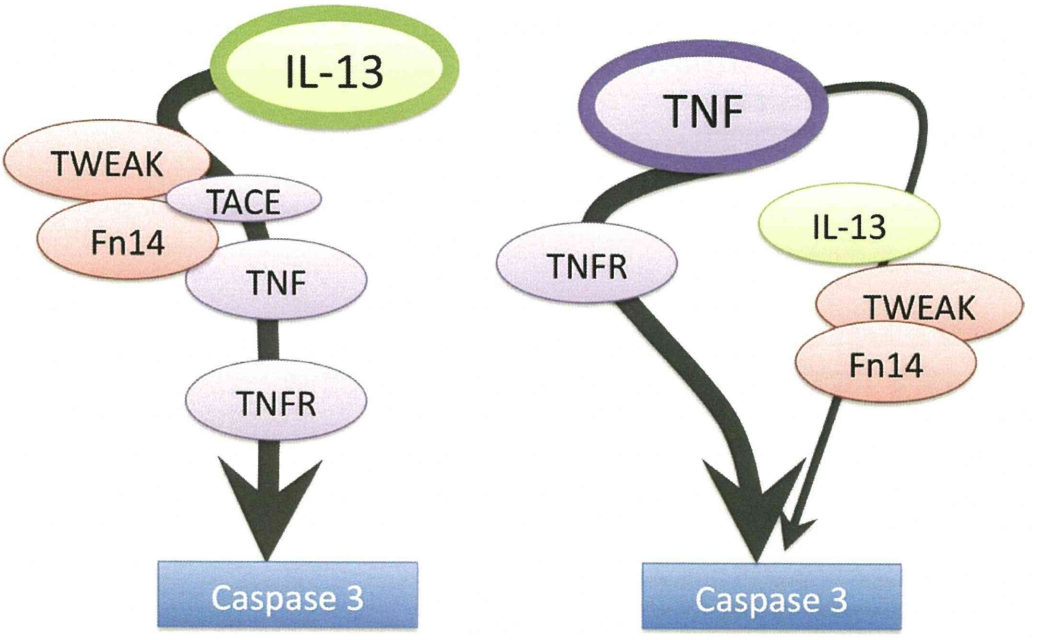

Supplementary Figure 5. Pathway of intestinal epithelial cell death by exogenous IL-13 and TNF-α. IL-13–induced caspase-3 activation is essentially dependent on endogenous TWEAK/Fn14, and TNF-α shedding induced by the action of TACE. Therefore, in the presence of IL-13, exogenous TNF-α or TWEAK are not necessary to induce apoptosis. Exogenous TNF-α is able to induce apoptosis in the absence of IL-13 or TWEAK/Fn14; however, the IL-13 and TWEAK/Fn14-dependent pathway is also involved in the early phase.

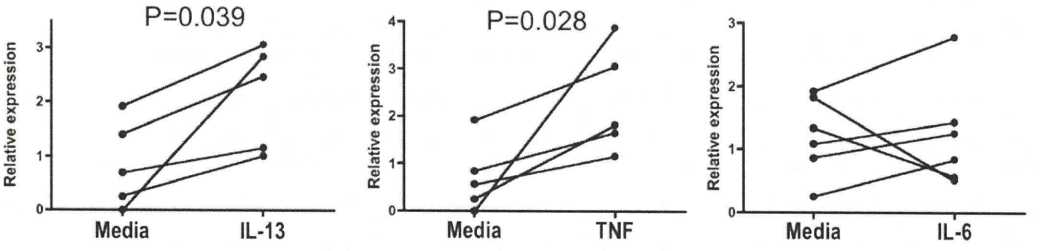

Supplementary Figure 6. Induction of Fn14 mRNA by cytokines. Fn14 relative expression values for primary mouse colon tissue cultured with media or indicated cytokine for 6 hours. Each *line* represents a culture from an individual mouse. Fn14 RNA levels were quantified by real-time PCR and normalized to GAPDH. Fn14 expression is shown as relative expression to the mean value for cultures with media alone. Paired *t* test was used for statistical analysis.

The EMBO Journal (2012) 31, 1904–1915 | © 2012 European Molecular Biology Organization | All Rights Reserved 0261-4189/12
www.embojournal.org

THE EMBO JOURNAL

NLK positively regulates Wnt/β-catenin signalling by phosphorylating LEF1 in neural progenitor cells

Satoshi Ota[1], Shizuka Ishitani[1], Nobuyuki Shimizu[1], Kunihiro Matsumoto[2], Motoyuki Itoh[3,4] and Tohru Ishitani[1,3,*]

[1]Division of Cell Regulation Systems, Department of Immunobiology and Neuroscience, Medical Institute of Bioregulation, Kyushu University, Fukuoka, Japan, [2]Group of Signal Transduction, Laboratory of Cell Regulation, Division of Biological Science, Graduate School of Science, Nagoya University, Nagoya, Japan, [3]Unit on Nervous Development Systems, Division of Biological Science, Graduate School of Science, Nagoya University, Nagoya, Japan and [4]Institute for Advanced Research, Nagoya University, Nagoya, Japan

Nemo-like kinase (NLK/Nlk) is an evolutionarily conserved protein kinase involved in Wnt/β-catenin signalling. However, the roles of NLK in Wnt/β-catenin signalling in vertebrates remain unclear. Here, we show that inhibition of Nlk2 function in zebrafish results in decreased Lymphoid enhancer factor-1 (Lef1)-mediated gene expression and cell proliferation in the presumptive midbrain, resulting in a reduction of midbrain tectum size. These defects are related to phosphorylation of Lef1 by Nlk2. Thus, Nlk2 is essential for the phosphorylation and activation of Lef1 transcriptional activity in neural progenitor cells (NPCs). In NPC-like mammalian cells, NLK is also required for the phosphorylation and activation of LEF1 transcriptional activity. Phosphorylation of LEF1 induces its dissociation from histone deacetylase, thereby allowing transcription activation. Furthermore, we demonstrate that NLK functions downstream of Dishevelled (Dvl) in the Wnt/β-catenin signalling pathway. Our findings reveal a novel role of NLK in the activation of the Wnt/β-catenin signalling pathway.

The EMBO Journal (2012) **31,** 1904–1915. doi:10.1038/emboj.2012.46; Published online 28 February 2012
Subject Categories: signal transduction; neuroscience
Keywords: lymphoid enhancer factor-1; nemo-like kinase; Wnt/β-catenin signalling; zebrafish

Introduction

The T-cell factor/lymphoid enhancer factor (TCF/LEF) family of transcription factors regulate Wnt/β-catenin signalling, which controls cell proliferation and fate decision during embryogenesis and adult tissue homeostasis (Logan and Nusse, 2004; Arce *et al*, 2006; Clevers, 2006; Hoppler and Kavanagh, 2007). TCF/LEF transcriptional activity is switched in a manner dependent on Wnt/β-catenin signalling (Logan and Nusse, 2004; Arce *et al*, 2006; Clevers, 2006; Hoppler and Kavanagh, 2007). In unstimulated cells, the levels of cytoplasmic β-catenin, a co-activator of TCF/LEF, are kept low by a degradation complex that includes Axin and glycogen synthase kinase 3β (GSK-3β). This kinase catalyses the phosphorylation of β-catenin, which promotes its ubiquitination and subsequent proteasomal degradation (Logan and Nusse, 2004; Clevers, 2006). In the absence of stimulation, TCF/LEF represses the expression of Wnt/β-catenin signalling-target genes by interacting with transcriptional co-repressors such as histone deacetylase 1 (HDAC1) and Groucho (Cavallo *et al*, 1998; Roose *et al*, 1998; Billin *et al*, 2000; Arce *et al*, 2009). The Wnt/β-catenin signalling pathway is induced when the secreted glycoprotein Wnt binds to the cell surface Frizzled (Fz) receptor and its co-receptor LRP5/6. This Wnt-bound receptor complex recruits the cytoplasmic protein Dishevelled (Dvl), which in turn brings the Axin–GSK-3β complex to the membrane and induces the phosphorylation of LRP6. Phosphorylated LRP6 promotes the dissociation of the β-catenin degradation complex (Davidson *et al*, 2005; Zeng *et al*, 2005, 2008). This series of events result in the accumulation of cytoplasmic β-catenin (Niehrs and Shen, 2010; MacDonald *et al*, 2011). The increased β-catenin concentration drives its migration into the nucleus where it forms complexes with TCF/LEF proteins, which then activate gene expression. However, the mechanism(s) by which TCF/LEF is converted from a repressor to an activator is poorly understood.

Nemo-like kinase (NLK) is an evolutionarily conserved MAP kinase-like kinase that regulates diverse signalling processes via phosphorylation of several transcription factors (Ishitani *et al*, 1999, 2010; Kanei-Ishii *et al*, 2004; Ohkawara *et al*, 2004; Kojima *et al*, 2005; Zeng *et al*, 2007). In *Caenorhabditis elegans*, the NLK homologue LIT-1 regulates POP-1, the *C. elegans* homologue of TCF/LEF (Meneghini *et al*, 1999; Rocheleau *et al*, 1999; Herman, 2001; Siegfried and Kimble, 2002; Siegfried *et al*, 2004). POP-1 represses the expression of genes required for endoderm induction. LIT-1 co-operates with the *C. elegans* β-catenin homologue WRM-1 to promote the phosphorylation and consequent nuclear export of POP-1, resulting in the transcriptional activation of POP-1-repressed genes (Meneghini *et al*, 1999; Rocheleau *et al*, 1999). LIT-1 also functions as a positive regulator of POP-1 in the fate specification of gonadal precursor cells (Herman, 2001; Siegfried and Kimble, 2002; Siegfried *et al*, 2004). However, the mechanism underlying this positive regulation is unclear. The regulation of POP-1 activity by LIT-1 is cell context dependent. The negative regulation of TCF/LEF by NLK has been also observed in human embryonic kidney 293 (HEK293) cells and the cervical epithelioid carcinoma cell line HeLa (Ishitani *et al*, 1999, 2003b). In these cell lines, overexpression of NLK inhibits β-catenin–TCF/LEF complex-mediated transcription via phosphorylation of TCF/LEF. On the other hand, positive regulation of TCF/LEF by NLK has not yet been observed in vertebrates.

*Corresponding author. Division of Cell Regulation Systems, Department of Immunobiology and Neuroscience, Medical Institute of Bioregulation, Kyushu University, 3-1-1 Maidashi, Higashi-ku, Fukuoka, Fukuoka 812-8502, Japan. Tel.: +81 92 642 6789; Fax: +81 92 642 6790; E-mail: tish@bioreg.kyushu-u.ac.jp

Received: 26 August 2011; accepted: 30 January 2012; published online: 28 February 2012

Mouse NLK is expressed in neural tissues, suggesting that mammalian NLK might play a role in nervous system development. Indeed, mice lacking NLK display various neurological abnormalities (Kortenjann *et al*, 2001). In the present studies, we demonstrate that NLK positively regulates the transcriptional activity of LEF1, a member of the TCF/LEF family, in zebrafish midbrain and mammalian neural progenitor cell (NPC)-like cell lines. We further show that Dvl activates NLK in the Wnt pathway and that NLK promotes the release of HDAC1 from LEF1 by phosphorylating LEF1. Our findings provide evidence that NLK mediates Wnt/β-catenin signalling, and consequently NPC proliferation through LEF1 phosphorylation.

Results

Nlk2 is essential for Wnt/β-catenin signalling in zebrafish midbrain

We used zebrafish as a model animal to investigate the roles of NLK in Wnt/β-catenin signalling *in vivo*. Zebrafish has two *nlk* genes, *nlk1* and *nlk2* (Supplementary Figure S1A and B). Nlk1 protein is more related to *Xenopus laevis* NLK1 (73% identical) than to human NLK (68% identical), while Nlk2 protein is most similar to human NLK (97% identical). Nlk2 and human NLK, but not Nlk1, contain histidine-rich (His-rich) and carboxyl terminal conserved regions (Supplementary Figure S1B). Vertebrate NLK proteins can be classified into two groups by phylogenetic analysis: type-I NLK, which includes *X. laevis* NLK1 and Nlk1, and type-II NLK, which includes mammalian NLK and Nlk2 (Supplementary Figure S1A). Recent studies show that Nlk1 regulates primary neurogenesis, ventrolateral mesoderm formation and brain anterior-posterior patterning in early embryogensis (Thorpe and Moon, 2004; Ishitani *et al*, 2010). We therefore investigated the physiological roles of Nlk2.

Expression of *nlk2* was observed in head tissues from the late somite stage (Figure 1A), suggesting that *nlk2* is involved in later brain development. To monitor activity of the zebrafish LEF1 homologue, Lef1, we used a transgenic zebrafish line carrying a Wnt/β-catenin signalling reporter construct (TOPdGFP), in which destabilized green fluorescent protein (dGFP) is driven by a promoter containing multiple TCF/LEF-binding sites, and thus indicates tissues where Lef1 is transcriptionally active (Dorsky *et al*, 2002). This transgenic zebrafish exhibited dGFP expression in the developing midbrain from the late somite stage (Figure 1B; Supplementary Figure S2A). As shown in Figure 1C, dGFP expression was observed in the dorsal and lateral marginal regions of the midbrain at 24 and 27 h.p.f. At 30 h.p.f., dGFP was expressed in the entire dorsal midbrain, while expression in lateral dorsal region was decreased. Consistent with this reporter activity, *lef1* and *nlk2* mRNAs were detected by *in-situ* hybridization in the entire dorsal midbrain of zebrafish embryos at 24 h.p.f. (Figure 1D). At 27 h.p.f., their expression levels in the lateral dorsal part of the midbrain were relatively low (Figure 1D) and their expression patterns were similar to that of TOPdGFP at 30 h.p.f. (Figure 1C). dGFP expression was attenuated by knockdown of zygotic Lef1 using a morpholino oligo (MO) that blocks *lef1* splicing (*lef1* spl MO) (Figure 1B; Supplementary Figure S2A and B; Supplementary Table SI), confirming that Lef1 indeed mediates the transactivation induced by Wnt/β-catenin signalling in the developing

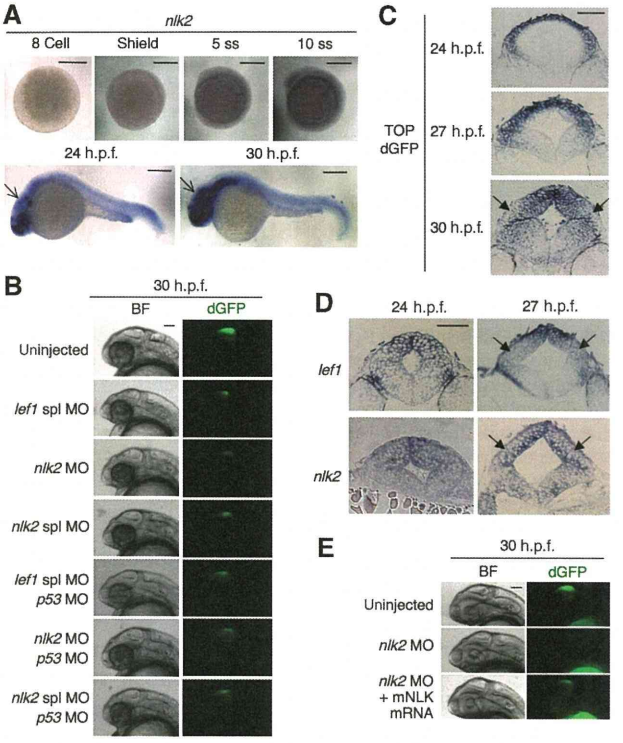

Figure 1 Nlk2 and Lef1 are required for the activation of Wnt/β-catenin signalling in zebrafish developing midbrain. (**A**) Whole mount *in-situ* hybridization staining for *nlk2* in zebrafish embryos at the indicated stage. Scale bar: 250 μm. The expression of *nlk2* in midbrain is indicated with arrows. (**B**, **E**) TOPdGFP-transgenic zebrafish embryos injected with *lef1* spl MO, *nlk2* MO, *nlk2* spl MO, or *p53* MO with or without mouse NLK (mNLK) mRNA, as indicated. Panels show the left side head views of 30 h.p.f. embryos with the anterior to the left. Cells expressing dGFP were visualized by fluorescence microscopy (right panels). Bright-field (BF) images are shown in left panels. Scale bar, 50 μm. Note that mNLK partially rescued *nlk2* MO-induced reduction of TOPdGFP activity ($n = 28$, 50%). (**C**, **D**) *In-situ* hybridization staining for TOPdGFP (**C**), *lef1* (**D**), and *nlk2* (**D**) in the transverse section at the level of midbrain in the indicated stage zebrafish embryos. Scale bar: 50 μm. The lateral dorsal region is indicated with arrows.

midbrain. We next examined the effect of *nlk2* inactivation on TOPdGFP reporter expression in the developing midbrain of zebrafish embryos using a translation-blocking MO against *nlk2* (*nlk2* MO) and an *nlk2* splice-blocking MO (*nlk2* spl MO) (Supplementary Figure S3). We found that, similarly to *lef1* spl MO-injected TOPdGFP fish embryos, the embryos injected with *nlk2* MO or *nlk2* spl MO showed lower TOPdGFP activity than the uninjected embryos at 24 h.p.f. (Supplementary Figure S2A and B; Supplementary Table SI) and 30 h.p.f. (Figure 1B; Supplementary Table SI). Co-injection of a validated MO for *p53* (Robu *et al*, 2007; Tsukada *et al*, 2010; Gerety and Wilkinson, 2011) together with an MO for *nlk2* or *lef1* had no effect on the phenotype induced by MO-mediated knockdown of *nlk2* or *lef1* (Figure 1B; Supplementary Table SI), eliminating the possibility that this phenotype was due to artificial MO-induced p53 activation (Robu *et al*, 2007). Furthermore, the *nlk2* MO-induced reduction of TOPdGFP activity in the midbrain was partially rescued by co-injection with mouse NLK mRNA (Figure 1E). We confirmed that injection of *lef1* spl MO or *nlk2* MO reduced dGFP expression levels in the midbrain but had no effect on the midbrain formation at 27 h.p.f. (Supplementary

Figure S2C). By observing the expression of brain maker genes, we also confirmed that neither injection of *nlk2* MO nor *lef1* spl MO affected the patterning of 24 h.p.f. zebrafish midbrain (Supplementary Figure S4A and B). These results suggest that Nlk2 positively regulates Wnt/β-catenin signalling in the developing zebrafish midbrain.

Nlk2 contribute to midbrain tectum development in zebrafish

To investigate the physiological roles of Nlk2 in the midbrain, we injected MOs for *nlk2* into a transgenic zebrafish line carrying the HuC:Kaede reporter, which expresses the fluorescent protein Kaede in neurons under the control of the neuron-specific *HuC/elavl3* promoter (Sato *et al*, 2006). Injection of either *nlk2* MO or *nlk2* spl MO reduced the size

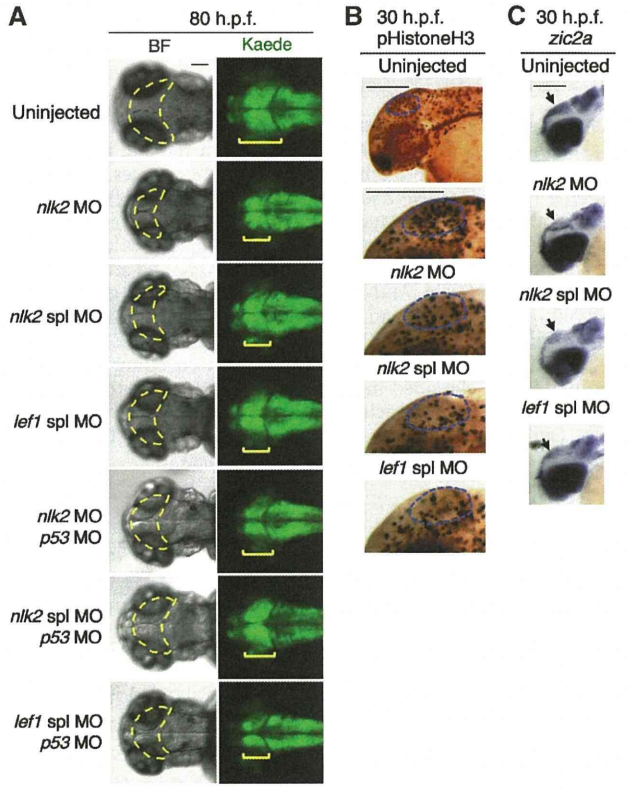

Figure 2 Nlk2 and Lef1 are essential for the midbrain tectum development in zebrafish. (**A**) HuC:kaede-transgenic zebrafish embryos injected with *nlk2* MO, *nlk2* spl MO, *lef1* spl MO, or *p53* MO as indicated. Panels show the dorsal head views of 80 h.p.f. embryos with the anterior to the left. Neurons expressing Kaede were visualized by fluorescence microscopy (right panels). Rectangles indicate the tectum. Bright-field (BF) images are shown in left panels. Broken lines indicate the tectum or presumptive tectal region. Scale bar, 50 μm. (**B**) Knockdown of either *nlk2* or *lef1* decreases the number of proliferating cells in midbrain. Anti-phospho-histone H3 immunostaining of 30 h.p.f. zebrafish embryos injected with *nlk2* MO, *nlk2* spl MO, or *lef1* spl MO, as indicated. Top panels show the left side head views of embryos with the anterior to the left. The other panels show the left side midbrain view of embryos with the anterior to the left. Broken lines indicate the presumptive tectal region. Scale bar, 250 μm. (**C**) Knockdown of either *nlk2* or *lef1* reduces expression of *zic2a* in midbrain. Panels show whole mount *in-situ* hybridization for *zic2a* in 30 h.p.f. embryos. Embryos were injected with *nlk2* MO, *nlk2* spl MO, or *lef1* spl MO as indicated. Panels show the left side head views of embryos with the anterior to the left. Expression of *zic2a* in midbrain is indicated with arrows. Scale bar, 250 μm.

of the midbrain tectum at 80 h.p.f. (Figure 2A; Supplementary Figure S5; Supplementary Table SI) but did not affect the development of the hindbrain (Supplementary Figure S5). Injection of *lef1* spl MO also resulted in a phenotype similar to that observed following injection of *nlk2* MOs. Co-injection of *p53* MO together with an MO for *nlk2* or *lef1* had no effect on the phenotype induced by MO-mediated knockdown of *nlk2* or *lef1* (Figure 2A; Supplementary Table SI). These results suggest that Nlk2 and Lef1 contribute to midbrain tectum development.

We next explored the mechanism by which Nlk2 and Lef1 contribute to tectum development. A previous report has shown that Lef1-mediated Wnt/β-catenin signalling promotes the proliferation of NPCs by activating the transcription of the *zic2a* and *zic5* genes in zebrafish developing midbrain (Nyholm *et al*, 2007). To examine whether Nlk2 contributes to the proliferation of midbrain NPCs, 30 h.p.f. zebrafish embryos were immunostained with anti-phospho-histone H3 antibody, which labels the nuclei of proliferating cells. Knockdown of *nlk2* or *lef1* decreased the numbers of phospho-histone H3-positive cells in the midbrain (Figure 2B; Supplementary Table SI), suggesting that Nlk2 and Lef1 are required for cell proliferation in the developing midbrain. We also found that expression of *zic2a* was decreased in the midbrain, but not in other regions of the brains of 30 h.p.f. embryos injected with *nlk2* MO, *nlk2* spl MO or *lef1* spl MO (Figure 2C; Supplementary Table SI). Using quantitative PCR (qPCR), we confirmed that injection of *nlk2* MO or *lef1* spl MO reduced the expression levels of *zic2a* in the midbrain (Supplementary Figure S2B). Our results suggest that Nlk2 and Lef1 promote the proliferation of NPCs through Wnt/β-catenin signalling in the developing midbrain.

Nlk2 phosphorylates Lef1 in zebrafish

We have previously reported that NLK phosphorylates human LEF1 at Thr-155 and Ser-166 *in vitro* (Ishitani *et al*, 2003b). The Thr residue is conserved between human and zebrafish (Figure 3A). To examine whether Nlk2 phosphorylates Lef1 at Thr-151, we generated an antibody that specifically recognizes phosphorylation of Lef1 at the conserved Thr residue (Figure 3A). This anti-phospho-Lef1 (anti-pLef1) antibody recognized Lef1 when it was co-expressed in mammalian neuro-2a cells with Nlk2, but not with kinase-negative Nlk2 (Figure 3B). These data suggest that Nlk2 phosphorylates Lef1 Thr-151. To verify antibody specificity, we generated a Lef1 mutation, Lef1(T151A), in which Thr-151 was changed to alanine. Lef1(T151A) was not detected by anti-pLef1 antibody when co-expressed with Nlk2 (Figure 3B).

We next investigated whether Nlk2 phosphorylates Lef1 in zebrafish embryos. We performed immunoblotting assays with anti-pLef1 and anti-Lef1 antibodies. Anti-Lef1 detected a protein of about 50 kDa in zebrafish embryo extracts (Figure 3C). In embryos injected with a translation-blocking MO against *lef1* (*lef1* MO) (Ishitani *et al*, 2005), levels of the protein detected by anti-Lef1 antibody decreased (Supplementary Figure S6), confirming that this protein corresponds to Lef1. Western blotting with anti-pLef1 antibody revealed that Lef1 phosphorylation could be detected in 24 h.p.f. embryo extracts (Figure 3C). Injection of *nlk2* MO reduced Lef1 phosphorylation, but had little effect on Lef1 protein levels. Thus, Nlk2 is able to phosphorylate Lef1 in 24 h.p.f. zebrafish embryos.

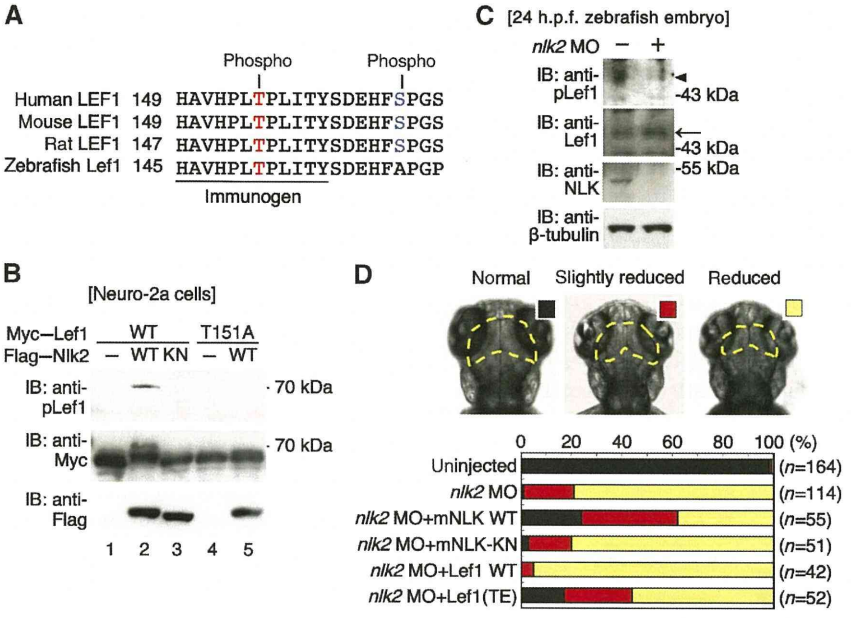

Figure 3 Nlk2 is involved in Lef1 phosphorylation in zebrafish. (**A**) Amino-acid sequence alignment of the NLK phosphorylation regions within vertebrate LEF1/Lef1 proteins. The Thr and Ser residues, which are phosphorylated by NLK, are indicated with red and blue letters, respectively. The bar under the sequence alignment indicates the immunogen for anti-pLef1 antibody. (**B**) Nlk2 phosphorylates Lef1 at the conserved Thr residue. Neuro-2a cells were transfected with Flag–Nlk2 wild-type (WT), Flag–Nlk2 kinase-negative mutant (KN), Myc–Lef1 (WT) and Myc–Lef1(T151A) as indicated. Cell lysates were immunoblotted with anti-pLef1, anti-Myc, and anti-Flag antibodies. (**C**) Nlk2 is required for phosphorylation of Lef1 at the conserved Thr residue in zebrafish. Zebrafish embryos were not injected or injected with *nlk2* MO, as indicated. Extracts were harvested from the embryos at 24 h.p.f., and immunoblotted with anti-pLef1, anti-Lef1, anti-NLK, and anti-β-tubulin antibodies. Arrow and arrowhead indicate Lef1 and phosphorylated Lef1 proteins, respectively. Anti-NLK antibody, which was generated in rabbit with a synthetic peptide corresponding to the carboxyl terminal conserved region of NLK, can recognize Nlk2, but not Nlk1. (**D**) The *nlk2* MO-induced tectum size reduction phenotype is rescued by expression of mouse NLK (mNLK) and zebrafish Lef1(T151E). Zebrafish embryos were injected with *nlk2* MO with or without transposase mRNA and Tol2-donor plasmid containing cDNA encoding mNLK-WT, mNLK-KN, Lef1-WT, or Lef1(TE), and then tectum size was determined. Embryos were classified into three groups based on the extent of tectum size reduction (normal, slightly reduced, and reduced). Upper panels show an example of each class. Broken lines indicate the tectum or presumptive tectal region. Lower graph shows the percentages of embryos exhibiting each class of tectum size reduction. The number shown in the right side of graph is the total number of embryos. Figure source data can be found in Supplementary data.

We examined whether Lef1 phosphorylation by Nlk2 is important for tectum development. Expression of mouse NLK, but not of kinase-negative NLK-KN, partially reversed the reduction in tectum size caused by *nlk2* MO in 80 h.p.f. *nlk2* morphants (Figure 3D). These results suggest that NLK determines tectum size in a manner dependent on its kinase activity. We then tested the effect of the Lef1(T151E) mutation, in which Thr-151 was replaced with glutamic acid to mimic phosphorylation at Thr-151. Expression of Lef1(T151E) partially reversed the reduction in tectum size caused by *nlk2* MO (Figure 3D). In contrast, wild-type Lef1 failed to suppress the *nlk2* MO-induced phenotype. These data suggest that Nlk2 regulates zebrafish tectum development via Lef1 phosphorylation.

Zebrafish has four *tcf* genes: *tcf7*, *tcf7l1a*, *tcf7l1b*, and *tcf7l2*, in addition to *lef1*. Among these *tcf* genes, *tcf7*, *tcf7l1a*, and *tcf7l2* were expressed in the Wnt/β-catenin signalling-active midbrain tissue (Supplementary Figure S7A). When co-expressed with Nlk2 in mammalian neuro-2a cells, Tcf7l1a and Tcf7l2, but not Tcf7 were recognized by the anti-pLef1 antibody (Supplementary Figure S7B). However, injection of a *tcf7l1a* splice-blocking MO (*tcf7l1a* spl MO) or a *tcf7l2* translation-blocking MO (*tcf7l2* MO) did not affect TOPdGFP activity in the midbrain of 24 h.p.f. embryos (Supplementary Figure S6C). These results suggest that Tcf7l1a and Tcf7l2 are not involved in Nlk2-mediated activation of Wnt/β-catenin signalling.

We next examined whether Wnt signalling regulates Lef1 phosphorylation and tectum development in zebrafish. The *wnt1* gene transcript was strongly expressed in 24 h.p.f. zebrafish dorsal midbrain (Supplementary Figure S4A and B), where the *nlk2* and the TOPdGFP reporter are also expressed. When *wnt1* was partially knocked down by MO in zebrafish embryos, Lef1 phosphorylation was reduced (Figure 4A). Furthermore, *wnt1* MO decreased TOPdGFP activity and *zic2a* expression at 24 h.p.f. (Figure 4B; Supplementary Figure S2B; Supplementary Table SII) and 27 h.p.f. (Supplementary Figure S2C), but had no effect on the expression of brain marker genes at 24 h.p.f. (Supplementary Figure S4C). Tectum size was also reduced in *wnt1* morphants at 80 h.p.f. (Figure 4C; Supplementary Figure S5; Supplementary Table SII). Expression of mouse Wnt-1 partially reversed the reduction in tectum size caused by *wnt1* MO (Figure 4C and D). Taken together, these results suggest that Wnt1 and Nlk2 regulate tectum development by inducing Lef1 phosphorylation in zebrafish midbrain.

NLK positively regulates Wnt/β-catenin signalling by phosphorylating LEF1 in NPC-like mammalian cell lines

The above results raised the possibility that NLK positively regulates Wnt/β-catenin signalling by phosphorylating Lef1 in zebrafish midbrain NPCs. We therefore examined the relationship between NLK and the Wnt/β-catenin pathway in the NPC-like mammalian cell lines, mouse neuroblastoma

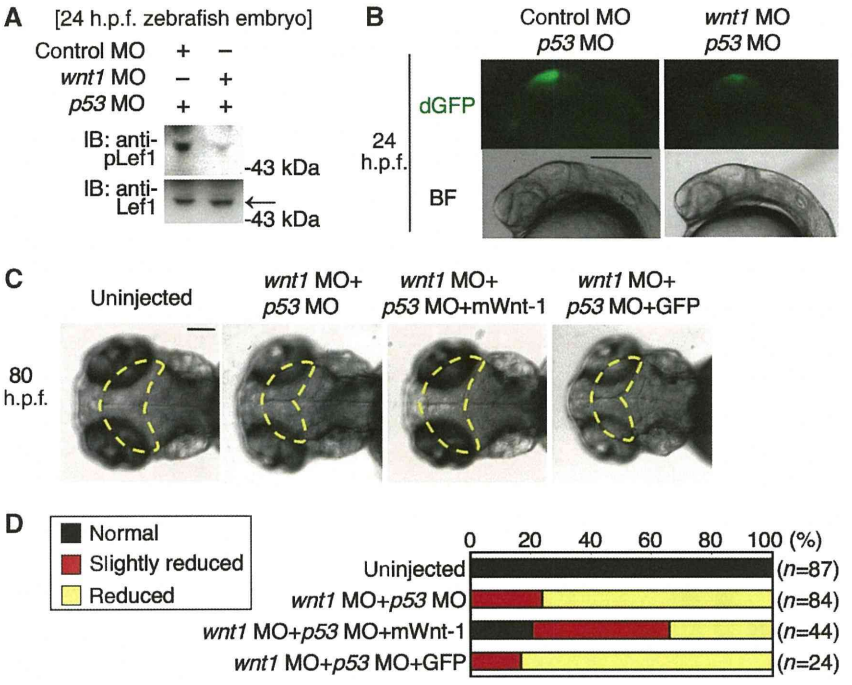

Figure 4 Wnt1 is involved in Lef1 phosphorylation in zebrafish. (**A**) Wnt1 is required for Lef1 phosphorylation at the conserved Thr residue in zebrafish. Zebrafish embryos were co-injected with *p53* MO and control MO or *wnt1* MO, as indicated. Extracts were harvested from the embryos at 24 h.p.f., and immunoblotted with anti-pLef1 and anti-Lef1 antibodies. (**B**) Wnt1 is required for activation of TOPdGFP in zebrafish midbrain. TOPdGFP-transgenic zebrafish embryos were co-injected with *p53* MO and control MO or *wnt1* MO, as indicated. Panels show the left side head views of 24 h.p.f. zebrafish embryos with the anterior to the left. Cells expressing dGFP were visualized by fluorescence microscopy (upper panels). Bright-field (BF) images are shown in lower panels. Scale bar, 250 μm. (**C**, **D**) Wnt1 is required for the formation of 80 h.p.f. zebrafish midbrain. Zebrafish embryos were injected with *p53* MO and *wnt1* MO with or without transposase mRNA and a Tol2-donor plasmid containing cDNA encoding mouse Wnt-1 (mWnt-1) or GFP, as indicated. Panels in (**C**) show a typical example. Broken lines indicate the tectum or presumptive tectal region. Embryos were classified into three groups based on the extent of tectum size reduction (normal, slightly reduced, and reduced). Graph in (**D**) shows the percentages of embryos exhibiting each class of tectum size reduction. The number shown in the right side of graph is the total number of embryos. Figure source data can be found in Supplementary data.

neuro-2a, and rat pheochromocytoma tumour PC12 cells. For this purpose, we used qPCR analysis and the reporter assay with a Wnt/β-catenin signalling-responsive reporter (TOPFLASH), which is driven by multiple TCF/LEF-binding sites (van de Wetering *et al*, 1997; Roose *et al*, 1998). TOPFLASH reporter activity was normalized against that of a reporter containing mutated TCF/LEF-binding sites (FOPFLASH). Deletion of the N-terminal region in β-catenin (β-cateninΔN) results in the accumulation of β-catenin, thus mimicking constitutive activation of Wnt/β-catenin signalling (Aberle *et al*, 1997). In HeLa and HEK293 cells, overexpression of β-cateninΔN alone induced relatively weak activation of the TOPFLASH reporter, while co-expression of β-cateninΔN with LEF1 strongly activated the reporter and enhanced the expression of *Axin2*, a direct target of Wnt/β-catenin signalling (Jho *et al*, 2002; Lustig *et al*, 2002; Supplementary Figure S8A–D). Consistent with a previous observation (Ishitani *et al*, 1999, 2003b), overexpression of NLK inhibited β-cateninΔN-LEF1-induced TOPFLASH reporter activity and *Axin2* expression in HEK293 and HeLa cells (Supplementary Figure S8A–D). In contrast, in neuro-2a and PC12 cells, β-cateninΔN overexpression or co-expression of β-cateninΔN with LEF1 did not activate the reporter (Figure 5A and B). However, we found that co-expression of NLK with β-cateninΔN and LEF1 efficiently activated TOPFLASH reporter activity in these cells and enhanced mRNA expression of Wnt/β-catenin signalling-target genes, such as *Axin2* and *cyclinD1* (Shtutman *et al*, 1999; Tetsu and McCormick, 1999), in a manner dependent on its kinase activity (Figure 5A and B; Supplementary Figure S8E and F). These results suggest that NLK kinase activity is required for promoting β-catenin–LEF1 complex-mediated activation of transcription in NPC-like cell lines.

We have previously reported that NLK inhibits β-catenin–LEF1 complex-mediated transcriptional activation by phosphorylating LEF1 at two conserved Thr and Ser residues (Figure 3A; Ishitani *et al*, 2003b). Consistent with this, NLK failed to inhibit β-cateninΔN–LEF1-induced TOPFLASH reporter activity when β-cateninΔN was co-expressed in HeLa cells with the LEF1-2A mutant, in which Thr-155 and Ser-166 were changed to alanines (Supplementary Figure S8A). We therefore tested the possibility that these sites are also involved in NLK-mediated Wnt/β-catenin signalling activation in neuro-2a and PC12 cells. We confirmed that NLK phosphorylates LEF1 at these residues in neuro-2a and PC12 cells. In SDS–PAGE gels, NLK induced a shift in the migration of wild-type LEF1, but not of the LEF1-2A mutant (Figure 5C). We next investigated the effect of the LEF1-2A mutation on NLK-dependent transcriptional activation. Compared with wild-type LEF1, co-expression of LEF1-2A with β-cateninΔN and NLK induced TOPFLASH reporter activity less effectively in neuro-2a and PC12 cells (Figure 5A and B). We next tested the LEF1-2E mutant, in which both Thr-155 and Ser-166 were changed to glutamic

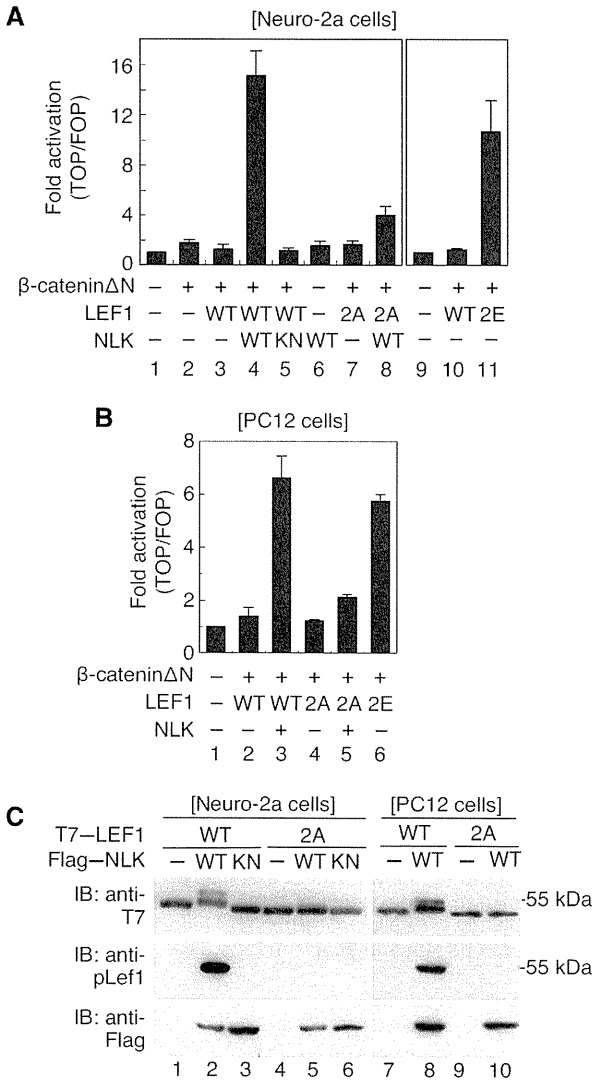

Figure 5 NLK promotes LEF1-mediated transcription in NPC-like mammalian cell lines. (**A**, **B**) The Wnt/β-catenin signalling reporter plasmids and expression plasmids encoding β-cateninΔN, human LEF1-WT, LEF1-2A, LEF1-2E, mouse NLK-WT, and NLK-KN were transfected as indicated and the luciferase activities were measured in neuro-2a (**A**) and PC12 (**B**) cells. (**C**) NLK phosphorylates LEF1 at Thr-155 and Ser-166 in neuro-2a and PC12 cells. Neuro-2a and PC12 cells were transfected with Flag-tagged mouse NLK (Flag–NLK-WT), Flag–NLK-KN, T7-tagged human LEF1 (T7–LEF1-WT) and T7–LEF1-2A mutant as indicated. Cell lysates were immunoblotted with anti-T7, anti-pLef1, and anti-Flag antibodies. Note that anti-pLef1 also recognized the phosphorylation of human LEF1. Figure source data can be found in Supplementary data.

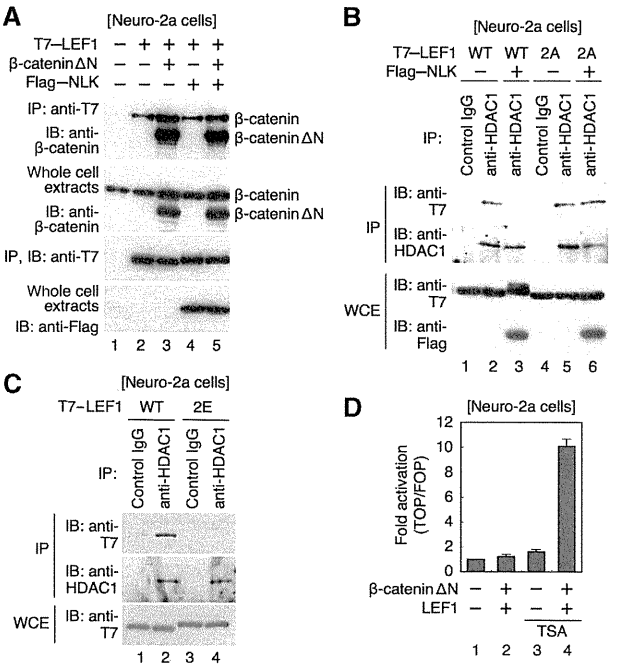

Figure 6 HDAC1 interacts with unphosphorylated LEF1. (**A**) NLK does not affect the interaction of LEF1 with β-catenin in neuro-2a cells. Neuro-2a cells were transfected with T7-tagged human LEF1, β-cateninΔN, and Flag-tagged mouse NLK as indicated. Cell extracts were subjected to immunoprecipitation with anti-T7 antibody. Immunoprecipitated complexes were immunoblotted with anti-β-catenin and anti-T7 antibodies. The amounts of β-catenin, β-cateninΔN, and Flag–NLK were confirmed by immunoblotting with anti-β-catenin and anti-Flag antibodies. (**B**, **C**) NLK-mediated LEF1 phosphorylation inhibits the interaction of HDAC1 with LEF1 in neuro-2a cells. Neuro-2a cells were transfected with plasmids encoding T7-tagged human LEF1-WT, T7–LEF1-2A, T7–LEF1-2E, and Flag-tagged mouse NLK as indicated. Cell extracts were immunoprecipitated with control IgG or anti-HDAC1 antibody. Immunoprecipitated complexes were immunoblotted with anti-T7 and anti-HDAC1 antibodies. The amounts of T7–LEF1 and Flag–NLK proteins were confirmed by immunoblotting with anti-T7 and anti-Flag antibodies, respectively. (**D**) Trichostatin A (TSA) treatment activates β-catenin–LEF1 complex-mediated transcription. Neuro-2a cells were transfected with Wnt/β-catenin reporter plasmids and plasmids encoding β-cateninΔN and LEF1. At 24 h after transfection, cells were left untreated or treated with 50 ng/ml TSA for 24 h and luciferase activity was measured. Figure source data can be found in Supplementary data.

acid to mimic phosphorylated threonine and serine. Co-expression of LEF1-2E with β-cateninΔN was able to activate the TOPFLASH reporter even in the absence of NLK overexpression (Figure 5A and B). These results suggest that LEF1 phosphorylation at Thr-155 and Ser-166 residues by NLK is important for its transcriptional activation of Wnt/β-catenin signalling in NPC-like mammalian cell lines.

NLK inhibits the interaction of LEF1 with HDAC1

We next examined how NLK promotes LEF1-mediated transcription in NPC-like mammalian cell lines. We have previously shown that NLK inhibits the DNA binding of TCF7L2 (also known as TCF4), a member of the TCF/LEF family (Ishitani *et al*, 1999, 2003b). Indeed, a ChIP assay in HeLa cells showed that NLK inhibited the binding of LEF1 to the *Axin2* regulatory element (Supplementary Figure S9A). We therefore examined the effect of NLK on the binding of LEF1 to the target genes in neuro-2a cells. NLK overexpression had no effect on LEF1 binding to the *Axin2* and *cyclinD1* regulatory elements (Supplementary Figure S9B). These results suggest that NLK affects LEF-1-mediated transcription in neuro-2a cells through some mechanism other than inhibition of its DNA-binding ability.

The transcriptional activity of LEF1 is regulated positively by β-catenin and negatively by co-repressors such as HDAC1 (Cavallo *et al*, 1998; Roose *et al*, 1998; Billin *et al*, 2000; Logan and Nusse, 2004; Clevers, 2006; Arce *et al*, 2009). As shown in Figure 6A, NLK overexpression had no effect on the interaction between LEF1 and β-cateninΔN. We therefore considered the possibility that NLK might relieve negative

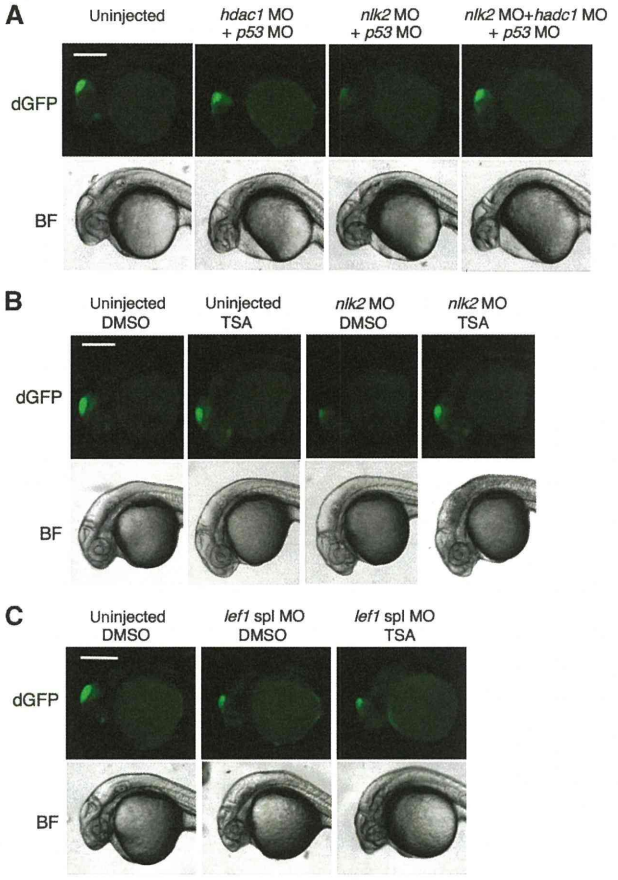

Figure 7 Nlk2 positively regulates Wnt/β-catenin signalling by blocking Hdac1-mediated inhibition in zebrafish midbrain. TOPdGFP-transgenic zebrafish embryos were uninjected or injected with *hdac1* MO, *nlk2* MO, *lef1* spl MO or *p53* MO at one-cell stage, as indicated. At 24 h.p.f., embryos were untreated (**A**) or left treated with DMSO or 1.2 μM TSA for 6 h (**B**, **C**). Panels show the left side head views of 30 h.p.f. zebrafish embryos with the anterior to the left. The cells expressing dGFP were visualized by fluorescence microscopy (upper panels). BF images are shown in lower panels. Scale bar, 250 μm.

regulation of LEF1. We found that LEF1 strongly interacted with endogenous HDAC1 in neuro-2a cells and that overexpression of NLK reduced this association (Figure 6B). We also found that the non-phosphorylated form of LEF1-2A stably interacted with HDAC1 regardless of NLK overexpression. In contrast, the LEF1-2E mutant that mimics constitutive phosphorylation failed to interact with HDAC1 (Figure 6C). Thus, HDAC1 binds preferentially to the unphosphorylated form of LEF1, and this interaction is disrupted by NLK-mediated phosphorylation. The above data raised the possibility that NLK promotes LEF1 activity by antagonizing HDAC1-mediated inhibition. To test this possibility, we examined the effect of trichostatin A (TSA), a specific inhibitor of HDAC1, on LEF1-mediated transcription in neuro-2a cells. Similarly to the effect of NLK overexpression (Figure 5A), TSA treatment strongly activated the TOPFLASH reporter in the presence of β-cateninΔN and LEF1 (Figure 6D).

It has been reported that the zebrafish HDAC1 homologue Hdac1 negatively regulates NPC proliferation mediated by Wnt/β-catenin signalling in zebrafish retina (Yamaguchi *et al*, 2005). In addition, *hdac1* transcripts are selectively expressed in the central nervous system (CNS), including the midbrain, at 24 h.p.f. (Cunliffe, 2004). We therefore investigated the possibility that Nlk2 positively regulates Wnt/β-catenin signalling by blocking Hdac1-mediated inhibition in zebrafish midbrain. Injection of *hdac1* MO or treatment with TSA reversed the reduction in Wnt/β-catenin signalling-induced TOPdGFP reporter activity observed in the midbrain of *nlk2* morphants (Figure 7A and B; Supplementary Tables SIII and SIV). In contrast, the *lef1* spl MO-induced phenotype was not suppressed by TSA treatment (Figure 7C; Supplementary Table SV). Thus, our results suggest that NLK/Nlk2 promotes LEF1/Lef1 activity by antagonizing HDAC1/Hdac1-mediated inhibition.

NLK functions downstream of Dvl in the Wnt signalling pathway in NPC-like mammalian cell lines

We examined whether Wnt-1 family proteins regulate NLK-mediated LEF1 activation in NPC-like mammalian cells. When PC12 cells were treated with Wnt-3a, a member of the Wnt-1 family of proteins, the TOPFLASH reporter was weakly activated (Supplementary Figure S10A). R-spondin 3, a member of the R-spondin family of secreted proteins, binds to a cell surface receptor of the Lgr family and facilitates Wnt-3a signalling by forming an Lgr/Fz/LRP complex (Carmon *et al*, 2011; de Lau *et al*, 2011). Treatment of PC12 cells with Wnt-3a and R-spondin 3 strongly activated the TOPFLASH reporter activity, and this activation was blocked by NLK siRNA treatment (Supplementary Figure S10A), suggesting that signalling by Wnt-3a and R-spondin 3 is transduced via NLK in PC12 cells. This combined treatment induced activation of NLK kinase activity (Figure 8A), phosphorylation of Lef1 (Figure 8B), and dissociation of HDAC1 from Lef1 (Figure 8C). The phosphorylation of Lef1 induced by Wnt-3a and R-spondin 3 was also inhibited by NLK siRNA (Figure 8B). These results suggest that Wnt-3a signalling activates the NLK kinase, which phosphorylates LEF1, resulting in its dissociation from HDAC1.

R-spondin promotes the Wnt/β-catenin pathway through LRP6 (Nam *et al*, 2006; Binnerts *et al*, 2007; Wei *et al*, 2007) and Dkk1 inhibits the Wnt/β-catenin signalling through an interaction with LRP6 (Bafico *et al*, 2001; Mao *et al*, 2001; Semënov *et al*, 2001). We found that expression of Dkk1 inhibited NLK activation induced by Wnt-3a and R-spondin 3 (Supplementary Figure S10B), suggesting that LRP6 is involved in the activation of NLK. Indeed, in PC12 cells, overexpression of constitutively active LRP6ΔN, which lacks the N-terminal extracellular domain (Brennan *et al*, 2004), activated the Wnt/β-catenin signalling reporter and this activation was reduced by NLK siRNA treatment (Supplementary Figure S11A).

Where in the Wnt signalling pathway does NLK function? Since it is known that Wnt signalling is transduced via Dvl (Logan and Nusse, 2004; Clevers, 2006), we investigated the relationship between Dvl and NLK in mediating Wnt signalling in PC12 and neuro-2a cells. In PC12 cells, overexpression of Dvl1 alone activated the Wnt/β-catenin signalling reporter and this activation was reduced by NLK siRNA treatment (Supplementary Figure S11A). In neuro-2a cells, Dvl1-induced reporter activation was relatively weak, but co-expression with LEF1 strongly enhanced reporter activity (Supplementary Figure S11B). This activation was blocked by NLK siRNA (Supplementary Figure S11B) or co-expression of the non-phosphorylated LEF1 mutant LEF1-2A (Supplementary Figure S11C). In addition, overexpression of Dvl1

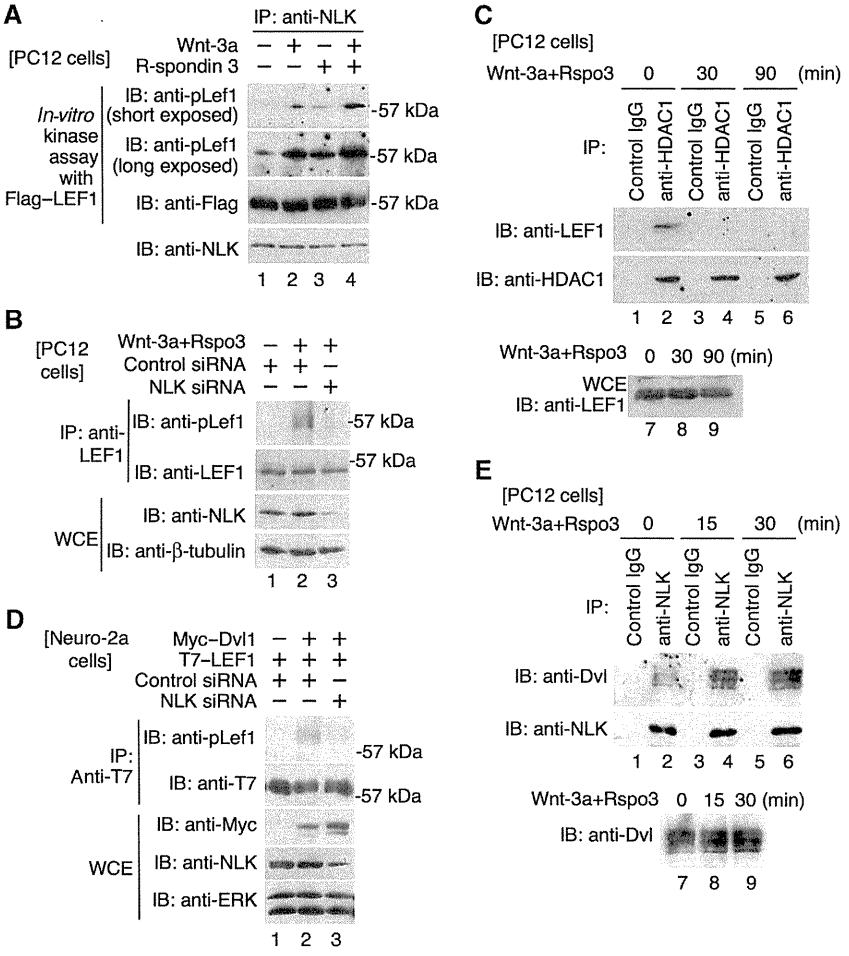

Figure 8 NLK functions downstream of Dvl in the Wnt/β-catenin signalling pathway. (**A**) Wnt-3a signalling activates the kinase activity of endogenous NLK. PC12 cells were untreated or treated with Wnt-3a and/or R-spondin 3 (Rspo3) for 30 min and endogenous NLK was immunoprecipitated (IP) with anti-NLK antibody. Aliquots of purified Flag–LEF1 and IP NLK proteins were subjected to a non-RI *in-vitro* kinase assay, and immunoblotted with anti-pLef1 antibody. Flag–LEF1 and NLK were confirmed by immunoblotting with anti-Flag and anti-NLK antibodies, respectively. (**B**) Wnt-3a signalling induces LEF1 phosphorylation. PC12 cells were treated with either control or NLK siRNA and then treated with or without Wnt-3a and Rspo3 for 30 min. Cell extracts were immunoprecipitated with anti-LEF1 antibody. IP complexes were immunoblotted with anti-pLef1 and anti-LEF1 antibodies. The amounts of endogenous NLK proteins were confirmed by immunoblotting with anti-NLK antibody. β-Tubulin was used as a loading control. (**C**) Wnt-3a signalling reduces the interaction of LEF1 with HDAC1. PC12 cells were treated with or without Wnt-3a and Rspo3 for the indicated time and then cell extracts were immunoprecipitated with control IgG or anti-HDAC1 antibody. IP complexes were immunoblotted with anti-LEF1 and anti-HDAC1 antibodies. The amounts of endogenous LEF1 were confirmed by immunoblotting with anti-LEF1 antibody. (**D**) Dvl1 induces LEF1 phosphorylation in a manner dependent on NLK. Neuro-2a cells transfected with Myc–Dvl1 and T7–Lef1 were treated with either control or NLK siRNA. Cell extracts were immunoprecipitated with anti-T7 antibody. IP complexes were immunoblotted with anti-pLef1 and anti-T7 antibodies. The amounts of Myc–Dvl1 and endogenous NLK were confirmed by immunoblotting with anti-Myc and anti-NLK antibodies, respectively. ERK was used as a loading control. (**E**) NLK binds to Dvl in a manner dependent on Wnt-3a signalling. PC12 cells were treated with or without Wnt-3a and Rspo3 for the indicated times and then cell extracts were immunoprecipitated with either control IgG or anti-NLK antibodies. IP complexes were immunoblotted with anti-Dvl and anti-NLK antibodies. The amounts of endogenous Dvl proteins were confirmed by immunoblotting with anti-Dvl antibody. Figure source data can be found in Supplementary data.

induced phosphorylation of exogenous LEF1 and this phosphorylation was blocked by NLK siRNA in neuro-2a cells (Figure 8D). Furthermore, we found that endogenous NLK associated with endogenous Dvl in PC12 cells and that Wnt-3a signalling enhanced this association (Figure 8E). The interaction of Dvl with NLK may activate its kinase activity. Taken together, these results suggest NLK functions downstream of Dvl in the Wnt signalling pathway in NPC-like mammalian cell lines.

Discussion

In the present study, we have shown that NLK positively regulates Wnt/β-catenin signalling in the developing midbrain of zebrafish and in NPC-like mammalian cell lines. In zebrafish, NLK-mediated signalling contributes to midbrain tectum development by promoting NPC proliferation. In NPC-like mammalian cells, Wnt-Dvl signalling activates NLK, which induces phosphorylation of LEF1, leading to its dissociation from HDAC1 and induction of LEF1 target gene expression.

The roles of zebrafish NLKs in Wnt/β-catenin signalling pathways

Zebrafish contains two NLK genes, *nlk1* and *nlk2*. A previous report has shown that Nlk1 is ubiquitously expressed from the early developmental stages and positively regulates